

1 **Multilevel regulation of the *glass* locus during *Drosophila* eye development**

2

3 Cornelia Fritsch<sup>1, #</sup>, F. Javier Bernardo-Garcia<sup>1,2, #</sup>, Tim-Henning Humberg<sup>1</sup>, Sara  
4 Miellet<sup>1</sup>, Silvia Almeida<sup>1</sup>, Armin Huber<sup>3</sup> and Simon G. Sprecher<sup>1</sup>

5

6 <sup>1</sup>Department of Biology, University of Fribourg, Chemin du Musée 10, 1700 Fribourg,  
7 Switzerland

8 <sup>2</sup>Department of Biochemistry and Biophysics, University of California, San Francisco,  
9 San Francisco, CA 94158, USA

10 <sup>3</sup>Institute of Physiology, University of Hohenheim, August-v.-Hartmann-Str. 3,  
11 Hohenheim, Germany

12 <sup>#</sup> These authors contributed equally to this work.

13

14 \* Correspondence: simon.sprecher@unifr.ch

15

16 Running title: Multilevel regulation of Glass

17 Keywords: *Drosophila*; visual system; CRISPR/Cas9; smORF; cis-regulation; eye  
18 development; photoreceptor determination; cell fate specification;

19

20

21 **ABSTRACT**

22 Development of eye tissue is initiated by a conserved set of transcription factors  
23 termed retinal determination network (RDN). In the fruit fly *Drosophila melanogaster*,  
24 the zinc-finger transcription factor Glass acts directly downstream of the RDN to  
25 control identity of photoreceptor as well as non-photoreceptors cells. Tight control of  
26 spatial and temporal gene expression is a critical feature during development, cell-  
27 fate determination as well as maintenance of differentiated tissues. The molecular  
28 mechanisms that control expression of *glass*, however remain largely unknown. We  
29 here identify complex regulatory mechanisms controlling expression of the *glass*  
30 locus. All information to recapitulate *glass* expression are contained in a compact 5.2  
31 kb cis-acting genomic element by combining different cell-type specific and general  
32 enhancers with repressor elements. Moreover, the immature RNA of the locus  
33 contains an alternative small open reading frame (smORF) upstream of the actual  
34 *glass* translation start, resulting in a small peptide instead of the three possible *glass*  
35 protein isoforms. CRISPR/Cas9-based mutagenesis shows that the smORF is not  
36 required for the formation of functioning photoreceptors, but to attenuate effects of  
37 *glass* misexpression. Furthermore, editing the genome to generate *glass* loci  
38 eliminating either one or two isoforms shows that only one of the three proteins is  
39 critical for formation of functioning photoreceptors, while removing the two other  
40 isoforms did not cause defects in developmental or photoreceptor function. Our  
41 results show that eye development and function is surprisingly robust and appears  
42 buffered to targeted manipulations of critical features of the *glass* transcript,  
43 suggesting a strong selection pressure to allow the formation of a functioning eye.

44

45

46 **INTRODUCTION**

47 While genes of the retinal determination network (RDN) are necessary and sufficient  
48 for inducing eye tissue in the imaginal-disc, distinct transcription factors are  
49 subsequently involved in promoting the developmental program of cell fate  
50 determination as well as terminal differentiaton. The zinc-finger transcription factor  
51 Glass provides a critical link between the RDN and terminal differentiaton. Glass is  
52 required during eye development for the differentiation of photoreceptor neurons,  
53 patterning of the ommatidia, as well as for the differentiation of cone- and pigment-  
54 cells [1-4]. *glass* mutants were first discovered by H.J. Muller in 1918 and O. L. Mohr  
55 in 1919, and were named after their smaller eyes with smooth, glassy surface and  
56 altered pigmentation [5]. While it was initially assumed that photoreceptor precursors  
57 undergo apoptosis in *glass* mutants, we recently showed that these cells adapt a  
58 neuronal cell fate, extend axons and form synapses, but fail to express *rhodopsins* as  
59 well as phototransduction genes. For the determination of photoreceptor idendity,  
60 *glass* promotes the terminal differentiation gene *hazy* [1, 6]. Intrestingly *glass* acts in  
61 conjunction with distinct transcripton factors to coordinate different cell fates during  
62 eye formation. For the specification of cone cells *glass* acts together with *dPax2*,  
63 *eyes absent* and *lozenge*, while for the formation of pigment cells it requires *escargot*  
64 [4]. Thus, dependent on the cellular context *Glass* is likely to control distinct  
65 developmental programs. However, mechanisms that act to control expression of  
66 *glass* remain largely unknown.

67 We here provide insight into surprisingly diverse regulatory mechanisms acting  
68 to regulate the *glass* locus. By further dissectioning a previously identified 5.2 kb  
69 genomic element we identified a set of regulatory core elements, including a general  
70 promotor, two pan-PR enhancer elements, a reciprocal enhancer element for non-PR  
71 cells, an element driving expression in a subset of PRs as well as an ocelli-specific  
72 enhancer element. By analysing a GFP reporter including the 5'UTR we identified an  
73 alterantive small open reading frame (smORF) upstream of the actual *Glass*  
74 translation start, resulting in a small peptide instead of the *Glass* protein. Interestingly  
75 editing the corresponding genomic sequences to mutate the smORF did not cause  
76 any developmental defect nor inference with physiological response of the retina nor  
77 photoattraction behaviour. However, when misexpressing *Glass* in a transcript  
78 including the smORF it attenuates developmental deficits, suggesting that while  
79 evolutionarily conserved within Drosophilids the smORF is not essential for eye

80 development, but may act to buffer Glass expression level. Moreover, we assessed  
81 the requirement and functionality of the three Glass protein isoforms by CRISPR-  
82 mediated genome editing introducing deletions into the *glass* locus resulting in the  
83 loss of one or two of the three isoforms. We analyzed these isoform mutants for the  
84 morphology of their eyes, the expression of photoreceptor markers that depend on  
85 Glass function, photoreceptor activity, and light preference behavior. We found that  
86 the short Glass PB isoform is not able to confer normal eye development and  
87 function resulting in a *glass* mutant phenotype, while the Glass PA isoform alone is  
88 fully functional. Our results suggest that the expression of *glass* is tightly regulated as  
89 the development of a functional tissue is surprisingly robust resulting in no detectable  
90 change in the physiological response or alteration in photoattraction behaviour upon  
91 deletion of the smORF. Similarly, only one of the isoforms is critical for eye  
92 development, suggesting that the other isoforms may function in a similar way to  
93 control levels of the functional protein. Since sequence comparison to closely related  
94 species show conservation of these features, such mechanisms may function to fine-  
95 tune gene expression.

96

## 97 **RESULTS**

98

### 99 **An overlapping upstream open reading frame inhibits the expression of a *glass* 100 reporter**

101 In the developing eye, expression of *glass* is initiated at the morphogenetic furrow in  
102 the eye-imaginal disc of third instar larvae and is detectable in the nuclei of all cells  
103 posterior to the morphogenetic furrow [7]. The same expression pattern is obtained  
104 with a reporter construct containing a 5.2 kb DNA fragment upstream of *glass* [8],  
105 spanning from -4190 bp to the AUG at +960 (Fig. 1A) [8]. Surprisingly, using this 5.2 kb  
106 upstream genomic sequence to drive a GFP reporter we observed GFP expression  
107 was barely detectable in the eye imaginal discs (Fig. 1B, B''). By increasing the gain  
108 at the confocal microscope, we were able to detect a weak GFP signal posterior to  
109 the morphogenetic furrow, barely above background level (Fig. 1B'', B'''). A closer  
110 inspection of our reporter construct revealed the presence of two potential start  
111 codons in the 5'UTR of *glass*, that were also present in the GFP reporter construct,  
112 one at position +889 relative to the predicted transcription start, the other at position  
113 +955. Translation from the first start codon, if functional, may compete with the GFP

114 start codon thus generating a protein that overlaps, but is not in frame, with the *GFP*  
115 coding sequence, resulting in the production of a 316 amino acid long protein (Fig.  
116 1B').

117 To test whether translation of GFP in our reporter construct was affected by  
118 the presence of the upstream start codon(s), we generated two additional reporter  
119 constructs: one, in which the potential upstream start codons were deleted (Fig. 1C'),  
120 and another, in which the GFP start codon was deleted and the GFP coding  
121 sequence was brought into frame with the upstream start codons (Fig. 1D'). Both  
122 GFP reporter variants resulted in strong GFP expression posterior of the  
123 morphogenetic furrow (Fig. 1C, C'', D, D''). Thus, the reduced GFP expression  
124 observed in the original reporter construct was caused by the translation of the  
125 reporter construct in a different reading frame due to the presence of additional start  
126 codons upstream of the GFP coding sequence. Since the GFP reporter we used  
127 does not contain a nuclear localization signal, GFP produced from its own start  
128 codon, as in construct C', is mainly localized in the cytoplasm (Fig. 1C'', C''').  
129 However, when GFP was fused in frame with the smORF, it showed strong nuclear  
130 localization (Fig. 1D'', D'''), suggesting that the first 24 amino acids added to the  
131 GFP coding sequence contain a nuclear localization signal. Indeed, amino acids 2 to  
132 20 of this fusion protein are predicted to affect nuclear localization [9]. Thus, the  
133 translation of this fusion protein starts at the first AUG codon at position +889.

134  
135 **Defined enhancer elements confine cell type specificity and temporal restricted  
136 expression**

137 In order to understand the *cis*-regulatory logic of *glass* expression we further  
138 dissected this genomic region in the construct that does not contain the two upstream  
139 start codons (Fig. 1C'). Using a number of restriction sites located in the upstream  
140 regulatory sequence, we generated truncations of our GFP reporter, similar to those  
141 used by Liu et al. [8], and also tested some deletions within this upstream sequence  
142 (Fig. 2A). After deleting half of the 5.2 kb fragment (construct B: -1885 to +886), GFP  
143 expression is still restricted to the region posterior of the morphogenetic furrow (Fig.  
144 2B, B'). Further deletion of a small fragment between the BamHI and EcoRI sites  
145 (construct C: -1598 to +886) shows patchy GFP expression in the developing  
146 photoreceptor precursors (Fig. 2C, C'). While construct B is expressed in all cell  
147 types forming the presumptive eye, the expression of construct C is restricted to

148 presumptive photoreceptor cells with variable expression levels (Fig. S1A),  
149 suggesting that the fragment from -1885 to -1598 might contain some non-  
150 photoreceptor specific enhancer. A fragment truncated at the XbaI site (construct D: -  
151 703 to +886) is expressed in all the photoreceptor precursors posterior of the  
152 morphogenetic furrow with the highest levels directly after the furrow and reduced  
153 levels towards the posterior end (Fig. 2D). This construct also shows ectopic  
154 expression in a stripe anterior of the furrow (Fig. D' arrowhead). This misexpression  
155 of GFP is spreading over the entire eye-antenna-disc in a construct starting at the  
156 XbaI site (construct E: -239 to +886, Fig. 2E, E'), suggesting that this fragment  
157 contains a minimal promoter whose activation is independent of eye specific  
158 enhancers. We used this minimal promoter region in combination with other  
159 fragments of the enhancer to analyse the expression patterns conferred by these 5'  
160 enhancer elements. We tested the 287 bp fragment between the BamHI and EcoRI  
161 sites that we suspected to drive expression specifically in non-photoreceptor cells  
162 based on the different expression patterns between constructs B and C. We found  
163 that this small fragment in combination with the minimal promoter (construct F: -1885  
164 to -1598 / -239 to +886) can restrict GFP expression to the region posterior to the  
165 morphogenetic furrow (Fig. 2F). With this enhancer fragment, the GFP signal is  
166 absent in the presumptive photoreceptor cells and restricted to the cells surrounding  
167 the photoreceptor precursors (Fig. 2F', Fig. S1B). A complementary construct lacking  
168 only this small region (construct G: -4301 to -1906 / -1598 to +886), shows a  
169 reciprocal expression pattern posterior of the furrow with expression restricted to  
170 presumptive photoreceptors (Fig. 2G,G'). The 1.2 kb region located at the 5' end of  
171 the *glass* enhancer fragment in combination with the minimal promoter (construct H: -  
172 4301 to -3123 / -239 to +886), also restricts GFP expression to cells posterior of the  
173 morphogenetic furrow (Fig. 2H). In this case GFP is only expressed in three of the  
174 eight presumptive photoreceptors (Fig. 2H'). We identified these as R2, R5, and R8  
175 using defined markers [10] (Fig. S1C). In addition, this part of the *glass* enhancer is  
176 required for expression in the ocelli anlage (Fig. 2G,H arrows). Finally, the fragment  
177 between the two BamHI sites (construct I: -3123 to -1906 / -239 to +886) drives GFP  
178 expression in all presumptive photoreceptors (Fig. 2 I,I', Fig. S1D), similar to  
179 construct D, but with lower expression levels directly after the furrow and increasing  
180 GFP levels towards the posterior end.

181        Taken together 5.2 kb *glass* regulatory region contains a general promoter  
182    region (-239 to +886), an ocelli enhancer region (-4301 to -3123, that also drives  
183    expression in a subset of photoreceptor precursors, a non-photoreceptor enhancer  
184    element (-1886 to -1598), and two general photoreceptor enhancer elements (-3123  
185    to -1906 and -1598 to -239).

186

187 **The overlapping upstream smORF is conserved and attenuates Glass  
188 misexpression**

189    The upstream start codons in the 5'UTR of *glass* strongly reduced the expression of  
190    our original GFP reporter construct, presumably due to interference with GFP  
191    translation and production of a 316 amino acid long protein encoded in the 3<sup>rd</sup> frame  
192    of the eGFP sequence used here. In the *glass* transcript, translation from the smORF  
193    might also interfere with Glass translation producing a 34 amino acid long peptide  
194    overlapping with the Glass coding sequence. Interestingly, the 4 nucleotide sequence  
195    preceding the upstream start codon (CAAG) is more similar to the *Drosophila*  
196    consensus Kozak sequence (MAAM, whereby M stands for either A or C) [11] than  
197    the sequence upstream of the actual Glass start codon (TGTC) (Fig. 3A). Sequence  
198    comparison with *glass* genes from other Diptera revealed that upstream start codons  
199    are present in all *glass* 5'UTRs of Drosophilidae as well as in *Lucilia*, *Musca*, and  
200    *Glossina*, possibly producing peptides that overlap with the Glass coding sequence  
201    (Fig. S2A). Although the length of these peptides differs slightly due to insertion and  
202    deletion of nucleotide triplets, the frameshift relative to Glass and the amino acid  
203    sequence are conserved within the Drosophilidae, suggesting that the encoded  
204    peptide itself might have a conserved function (Fig. S2B). Interestingly, the N-  
205    terminal half of the peptide contains mainly basic residues that can provide a nuclear  
206    localization signal, as revealed in the GFP reporter construct that was cloned in  
207    frame with the upstream start codon (Fig. 1D). The central part of the peptide  
208    sequence is more variable and truncated in *D. grimshawi*, *D. virilis*, and *D.*  
209    *mojavensis*, while it is extended in *D. wilistoni*, *L. cuprina*, *M. domestica*, and *G.*  
210    *morsitans* (Fig. S2B). Not surprisingly, conservation is also high in the C-terminal part  
211    overlapping the Glass coding sequence. The N-termini of the Glass orthologs of  
212    other insects, including mosquitoes, are not conserved, and there are no upstream  
213    overlapping open reading frames in these transcripts.

214 Since the 34 amino acid long peptide is encoded by the *glass* mRNA, it might  
215 have a function in eye development. We used the CRISPR/Cas9 technique to  
216 introduce small deletions in the peptide coding sequence that will result in a  
217 frameshift of the peptide without affecting the Glass coding sequence. We named the  
218 resulting smORF alleles “*brainy smurf*” (*brs*) after the smurf with the glasses. We  
219 introduced a double strand break 6 nucleotides downstream of the start codon of the  
220 peptide and provided a template for repair that contained a single nucleotide change  
221 as well as a single nucleotide deletion (*brs*<sup>-1nt</sup>) (Fig. 3A). We crossed the G0 flies to  
222 flies that had a deficiency of the *glass* locus and selected offspring that showed a  
223 subtle rough eye phenotype over these deficiencies. In addition to the single  
224 nucleotide deletion provided by the template, we also found several lines that had  
225 small indels in the region of the CRISPR site used (Fig. S3A). We used *w*<sup>1118</sup> flies as  
226 controls, since most of our *brs*<sup>-</sup> lines were in a *w* background due to crossing the G0  
227 flies with *w*; *Df(3R)Exel6178* and the F1 flies with *w*; *Dr e/TM3*. *w*<sup>1118</sup> control flies  
228 have big round compound eyes expressing the phototransduction proteins  
229 Rhodopsin1 (Rh1), No receptor potential A (NorpA), Transient receptor potential  
230 (Trp), and Transient receptor potential-like (Trpl) (Fig. 3B). Adult flies are attracted to  
231 light in phototaxis experiments [6]. This is also the case for white eyed mutants (Fig.  
232 3B). *brs*<sup>-1nt</sup> homozygous flies have normal eyes, expressing all tested markers and  
233 show light preference comparable to wildtype flies (Fig. 3C). We observed the same  
234 phototaxis behaviour and marker gene expression in the randomly generated *brs*  
235 mutations (Fig. S3B-F).

236 The GFP reporter constructs demonstrated that the presence of the upstream  
237 start codon can interfere with translation from the actual start codon. To test if this is  
238 also the case for the translation of Glass, we introduced a 5 nucleotide deletion at the  
239 Glass start codon, putting it into frame with the upstream start codon (*brs*<sup>-5nt::Glass</sup>)  
240 (Fig. 3A). In this case, Glass translation starts at the upstream start codon that has  
241 the “better” Kozak sequence and fuses the nuclear localization signal encoded by the  
242 N-terminus of Brs to the Glass protein. We considered that this could result in higher  
243 levels of Glass activity that might interfere with eye development. However, we did  
244 not observe any changes in marker gene expression, photoreceptor shape, or light  
245 preference (Fig. 3D). Thus, the potential increase of Glass protein either does not  
246 interfere with its function, or is compensated by other mechanisms.

247 To test our hypothesis that the upstream start codon might interfere with Glass  
248 translation, we used an over-expression assay. Driving *UAS-glass-PA* expression  
249 with a strong *eyeless*-Gal4 enhancer results in lethality of the pharate flies (Fig. 3E,  
250 Table1). The flies have severe head defects that prevent them from eclosing with  
251 only a small number of escapers (0.4%) (Fig. 3F). Overexpression of a *UAS-brs*  
252 construct did not affect viability of the flies or their eye shape (Fig. 3G, Table 1),  
253 indicating that the small peptide produced does not interfere with eye development.  
254 Co-expression of *UAS-glass-PA* and *UAS-brs* inserted on different chromosomes  
255 showed a similar level of lethality as *UAS-glass-PA* alone (0,3% survival rate),  
256 indicating that the peptide itself does not interfere with Glass function. However, in a  
257 construct that contains the peptide coding sequence upstream and overlapping with  
258 the Glass PA coding sequence as in the endogenous transcript, the lethality caused  
259 by the over-expression of Glass protein was reduced, resulting in a 20.3% survival  
260 rate, where the adult escapers had normal or smaller eyes (Fig. 3H). Therefore, the  
261 presence of the Brs peptide itself does not reduce Glass levels. *brs* only interferes  
262 with Glass translation, when directly placed as an upstream overlapping open  
263 reading frame in the *glass* mRNA.

264

265 **The Glass PA protein isoform by itself is sufficient for photoreceptor  
266 differentiation and function**

267 *glass* encodes a 604 amino acid protein containing a transcriptional activation  
268 domain and a DNA-binding domain that consists of five zinc-fingers of which the  
269 three C-terminal zinc-fingers were shown to be necessary and sufficient for DNA  
270 binding [7, 12]. According to FlyBase (flybase.org), the *glass* gene encodes three  
271 different protein isoforms (Fig 1A). The PA isoform contains a complete set of 5 zinc-  
272 fingers providing sequence specific DNA binding to the target genes of Glass [3, 13].  
273 In addition to the Glass PA isoform, two other isoforms are predicted to exist based  
274 on expressed sequence tags and sequence conservation [14, 15]. Failure to splice  
275 out the last intron of the mRNA transcript, results in the production of a truncated 557  
276 amino acid Glass PB isoform lacking the second half of the fifth zinc-finger. This  
277 version of Glass cannot bind specifically to its target sequence *in vitro* [12]. Of the 19  
278 cDNA clones whose sequences are available on FlyBase (flybase.org), seven are  
279 covering the last and/or the second-last exon, and all seven still contain the last  
280 intron, suggesting that this intron is frequently retained in the transcript. The position

281 of the last intron (intron 4 in *Drosophila*) including the stop codon immediately  
282 following the exon-intron junction is only present in the *glass* orthologs of Diptera and  
283 Lepidoptera Fig. S4A). In the postman butterfly (*Heliconius melipone*) the stop codon  
284 is not located immediately after the exon intron junction but 17 basepairs into the  
285 intron. Other arthropods do not have an intron at this position.

286 An extended 679 amino acid long Glass PC isoform, containing all 5 zinc-  
287 fingers followed by additional 75 amino acids, is produced by a readthrough of the  
288 Glass PA stop codon. The prediction of this longer isoform is based on sequence  
289 conservation 3' of the regular stop codon [16]. A comparison of the sequence  
290 following the Glass stop codon within the higher *Diptera* shows conservation on the  
291 amino acid level suggesting that the extended protein is produced by a direct  
292 misinterpretation of the stop codon without shifting the reading frame (Fig. S4B). The  
293 amino acid sequences of the extended Glass proteins from different higher *Diptera*  
294 are highly conserved at their N- and C-termini, but have a central region that is rich in  
295 histidine residues of very variable length. Particularly the *Musca* and *Lucilia* Glass PC  
296 versions contain a high number of additional amino acids in this central part. The PC  
297 sequence is not conserved in other insects including mosquitoes.

298 To test the requirement and function of the three different Glass isoforms *in*  
299 *vivo*, we introduced specific changes in the endogenous *glass* locus by  
300 CRISPR/Cas9- mediated genome editing, eliminating either one or two of the Glass  
301 isoforms (Fig. 4A). We used *w<sup>1118</sup>* flies as controls, since our *glass* deletion lines  
302 were in a *w* background due to crossing the G0 flies with *w;; Df(3R)Exel6178* and  
303 the F1 flies with *w;; Dr e/TM3* (Fig. 4B). Flies expressing only the Glass PA+PC  
304 isoforms due to a deletion of the last intron had normal, functional eyes expressing  
305 phototransduction proteins like control flies (Fig. 4C). In contrast, a deletion that  
306 allowed only the production of the truncated PB isoform phenocopied *glass* amorphic  
307 mutations, in which photoreceptors failed to differentiate as revealed by the loss of  
308 phototransduction proteins (Fig. 4D) [1]. We also prevented the production of the PC  
309 isoform by adding two additional stop codons at the end of the Glass PA sequence.  
310 This had no effect on eye shape or on photoreceptor marker gene expression (Fig.  
311 4E). By deleting the last intron and adding stop codons at the end of the Glass PA  
312 sequence we generated flies that can only express the PA isoform. These flies also  
313 have normal functional eyes expressing all tested markers (Fig. 4F). In addition to  
314 marker gene expression, we also measured photoreceptor activity by recording

315 electroretinograms (ERGs). We found that all isoform mutants that had normal eye  
316 shape and were expressing phototransduction proteins, showed normal ERG  
317 responses [17], while the flies expressing only the Glass PB isoform did not produce  
318 any ERG signal in response to light (Fig. 4G). When we tested the light preference of  
319 our different Glass isoform mutants, we found that all variations expressing the Glass  
320 PA isoform showed light preference comparable to wildtype flies (Fig. 4H). In contrast,  
321 the flies expressing only the Glass PB isoform were photoneutral, with a light  
322 preference index that is not significantly different from chance, but significantly  
323 different from that of control flies and similar to that of *glass* mutants, which fail to  
324 detect light [6]. A *glass* mutant phenotype was also observed in flies in which, after  
325 CRISPR-induced DNA double strand break, the DNA repair occurred in form of non-  
326 homologous end joining, either deleting the exon-intron junction and the stop codon  
327 located in the last intron, or introducing a frameshift at the beginning of the last exon  
328 (Fig. S5A). Like flies expressing the truncated Glass PB isoform, these flies also  
329 have small eyes with a glassy surface. They do not express any of the tested PR  
330 makers, have no ERG response and do not show phototaxis behaviour (Fig. S5B-G).

331 Thus, although conserved, the extended version of Glass is dispensable in  
332 photoreceptors. In contrast, the truncated PB version alone cannot fulfil Glass  
333 function, while its absence does not interfere with Glass function in the eye.

334

335

## 336 **DISCUSSION**

337 Changes of the genomic context in a given locus can have a profound influence on  
338 gene expression. Addition or deletion of transcription factor binding sites does not  
339 only affect when and where a gene is transcribed, but can also determine the  
340 expression level. The addition of an exon containing a start codon upstream of the  
341 first coding exon can result in an N-terminal extension of the protein if the start codon  
342 is in the same reading frame as the coding sequence, or it might interfere with  
343 translation if it is in a different reading frame. Insertion of an intron within the coding  
344 sequence can result in the production of a truncated protein due to intron retention.  
345 Stop codon readthrough can lead to the production of an elongated version of the  
346 protein. Such changes can reduce the protein levels or even alter protein function  
347 meaning that they are usually quickly removed from the genome. Thus, conservation  
348 of such traits over more than the most closely related species indicates that they are

349 neutral or even beneficial. The *Drosophila* transcription factor *glass* combines such  
350 features in its transcript, making it a good candidate to investigate these phenomena  
351 in the well studied context of photoreceptor development and function. Here we  
352 identified an upstream overlapping open reading frame affecting Glass translation.  
353 We analysed the role of the different Glass isoforms generated by intron retention  
354 and stop codon readthrough. In addition, we dissected the *glass* regulatory sequence  
355 and identified several cell- and tissue specific enhancer elements.

356

357 **General and cell-specific enhancer elements regulate *glass* expression**

358 The 5.2 kb region upstream of the *glass* start codon had previously been identified as  
359 the minimal sequence required for normal Glass expression [8]. The lacZ-reporter  
360 construct used in this paper also contained the upstream start codon located in intron  
361 2. Due to the enzymatic activity of the  $\beta$ -galactosidase sufficient signal was produced  
362 to detect reporter gene activity posterior of the morphogenetic furrow. However,  
363 further truncations of the upstream sequence only yielded transgenic lines with weak  
364 or variable expression or lines that did not show expression at all. Similarly, our  
365 original GFP-reporter construct showed only very weak expression levels even with  
366 the same 5.2 kb enhancer fragment. After removal of the upstream start codon,  
367 expression of our GFP-reporter construct was strongly enhanced allowing us to  
368 perform a classical enhancer bashing approach to further dissect the upstream  
369 region of *glass*. We were able to identify different enhancer regions that conferred  
370 reporter gene expression in cells posterior to the morphogenetic furrow. The retinal  
371 determination network consisting of several transcription factors, specifies the  
372 position of the eye field in many different organisms [18]. Sine oculis, a member of  
373 the retinal determination network regulates *glass* expression by directly binding to  
374 sites in the enhancer sequence [1]. The three Sine oculis binding sites tested in this  
375 paper are located in the BamHI-EcoRI fragment (-1885 to -1598). However, many  
376 additional potential Sine oculis binding sites are spread along the entire 5.2 kb  
377 upstream sequence (altogether 10 sites with a perfect AGATA<sub>C</sub> consensus  
378 sequence and 22 sites with a more degenerate version YGATA<sub>Y</sub>). Given that all  
379 enhancer fragments we tested, showed GFP expression posterior to the  
380 morphogenetic furrow, we propose that Sine oculis binds to multiple sites in the 5.2  
381 kb enhancer to activate *glass* expression. In addition to this general reporter gene  
382 activation we identified specific enhancer regions driving expression in distinct cell

383 types. For example, the 5'-end of the enhancer that leads to expression in the ocelli  
384 anlage and in a subset of the photoreceptors, or the BamHI-EcoRI region that  
385 activates expression in non-photoreceptor cells. Thus, other transcription factors  
386 binding more specifically to these enhancer elements, might regulate *glass*  
387 expression in a cell-type dependent manner.

388

389 **The extended Glass PC isoform is dispensable for eye development and**  
390 **function**

391 Stop codon readthrough is relatively abundant in *Drosophila* [19]. Especially genes  
392 expressed in the nervous system are putative candidates for this process [20]. Glass  
393 has also been listed as a candidate for this protein extension mechanism based on  
394 several criteria [16]: Sequence comparison of the amino acids following the regular  
395 stop codon shows a higher conservation within higher Diptera than what is found in  
396 the 3'UTR of non-readthrough transcripts. The pattern of nucleotide substitutions also  
397 suggests that there is no alteration of the reading frame as it might occur in the case  
398 of alternative splicing or ribosome hopping. The most frequent stop codon  
399 readthrough context (UGAC) [16], is also found at the Glass PA stop codon. Upon  
400 readthrough of a UGA stop codon either arginine, cysteine, serine, or tryptophane  
401 can be inserted by a near-cognate tRNA at this position [21]. In our isoform deletion  
402 experiments we did not test the conditions at which the stop codon is deleted or  
403 replaced by another codon (Glass PC and Glass PB+PC) because the function of the  
404 resulting protein might be affected by the type of alteration we introduce. Our results  
405 from the mutants expressing only the Glass PA isoform suggest, that under  
406 laboratory conditions, stop codon readthrough and production of the extended Glass  
407 PC version is not required for eye development and photoreceptor function.

408

409 **Splicing of intron 4 is required to produce functional Glass protein**

410 The Glass PB isoform alone is not functional. Our deletion mutants that can only  
411 express this truncated version as well as our other deletions that affect splicing and  
412 result in proteins terminating in intron 4, have a *glass* mutant eye phenotype, that is:  
413 they lack the expression of photoreceptor markers, show no photoreceptor activity  
414 and are photoneutral [1, 6, 22]. This corroborates previous results that showed that  
415 the last three zinc-fingers are essential for sequence specific DNA-binding and that a  
416 Glass protein lacking the C-terminal end shows no transcriptional activity [12]. The

417 intron that is retained in the Glass RB transcript, is only found in Diptera and  
418 Lepidoptera, suggesting that it originated in the last common ancestor of flies and  
419 butterflies. Intron retention can be a means of regulating protein levels since they are  
420 usually degraded by nonsense-mediated decay [23]. One of the first examples for  
421 cell-type specific intron retention was the *Drosophila* P-element [24]. In germ cells  
422 intron 3 is spliced out resulting in functional transposase production. In contrast, in  
423 somatic cells intron 3 is retained resulting in a truncated protein that antagonizes the  
424 full-length protein. Intron retention can also generate new protein isoforms like the  
425 *Drosophila* Noble protein [25]. In addition, intron-retaining mRNA transcripts can  
426 remain in the nucleus and be spliced upon requirement providing a source of  
427 transcript that could be faster activated than by de novo transcription [26]. Recent  
428 RNAseq data suggests that intron 4 is not retained in the *glass* mRNA [4]. The  
429 authors found that expression of either the *glass* RA+RC or the *glass* RB transcript  
430 from transgenic constructs resulted in production of functional Glass protein,  
431 suggesting that in their ectopic expression experiments, intron 4 of the RB transcript  
432 was spliced out to produce full-length Glass PA (and PC) protein. Thus, we would  
433 consider the *glass* RB transcript as an intermediate stage that has been accumulated  
434 during cDNA preparation but that can be further processed to encode functional  
435 Glass protein. As we show here, the absence of intron 4 in the *glass* gene allowing  
436 only the production of the Glass PA (and PC) protein does not affect eye  
437 development and function.

438

#### 439 **Brs interferes with Glass translation**

440 According to the scanning model of translation initiation [27], the 40S ribosomal  
441 subunit scans the mRNA from the 5'end until it encounters the first AUG codon.  
442 Translation will start at this codon, which in the case of *glass* mRNA would mean that  
443 only the Brs protein should be produced. However, under certain conditions,  
444 translation can also start at a later AUG codon [28]. One of these mechanisms, called  
445 leaky scanning, applies for an upstream AUG with a weak context, were the codon  
446 with the weak context is skipped by some ribosomes starting translation further  
447 downstream. However, this cannot be the case for Glass translation, since there are  
448 two AUG codons upstream of the Glass start codon within exon 2 and both have a  
449 better Kozak sequence than the actual Glass AUG. Another mechanism would be  
450 reinitiation, where after translation of a small upstream open reading frame, the

451 ribosome can move on and re-acquire a Met-tRNA allowing it to reinitiate translation  
452 at the next AUG codon. However, since ribosomes cannot backup, the overlapping  
453 open reading frame should profoundly inhibit Glass translation [29, 30]. It was shown  
454 that overlapping upstream open reading frames; and particularly those that have an  
455 optimal AUG context, are efficiently removed from the *Drosophila* genome [31],  
456 suggesting that those that can be found and that are even conserved outside of the  
457 most closely related species, have been selected due to a specific function. In the  
458 case of Glass, we found evidence that translation from the upstream start codon  
459 strongly reduces GFP translation and also interferes with Glass translation when  
460 overexpressed. However, this suggests that the endogenous Glass protein would be  
461 expressed at very low levels. One possible way to overcome this problem, would be  
462 by splicing out exon 2 so that the two upstream AUGs and the Glass AUG would be  
463 removed from the transcript. In this case translation would start from an AUG codon  
464 in exon 3 (amino acid 26 of the predicted full length protein). However, there is no  
465 evidence, that exon 2 is spliced out of the transcript to produce a truncated Glass  
466 version. Another hypothesis would be that Glass translation starts by reinitiation at  
467 the AUG codon in exon 3 after translation of Brs. In fact, the Glass proteins of  
468 *Anopheles darlingi* and of *Culex quinquefasciatus* are predicted to start at this  
469 position (with a conserved motif: MYISC), while *Anopheles gambiae* Glass is  
470 predicted to start in an exon located further upstream of the start codons of the other  
471 two mosquito species, but with an N-terminal sequence that is not related to that  
472 found in *Drosophila* and other higher Diptera. Also, other insects' Glass proteins start  
473 further downstream than in the Diptera. It could be possible that for most insects the  
474 actual Glass translation start has not yet been identified due to higher sequence  
475 divergence at the N-termini. This would suggest, that the first 25 amino acids mostly  
476 encoded by exon 2 of the *Drosophila* transcripts are dispensable for Glass function,  
477 or that they are only required in higher Diptera. In addition to regulating Glass protein  
478 levels by directly interfering with translation efficiency, the Brs peptide could have  
479 other functions in the developing eye, where it is expressed along with Glass. Small  
480 peptides can have important roles such as hormones, pheromones, transcriptional  
481 regulators, antibacterial peptides, etc. [32]. However, we could neither identify such a  
482 role for Brs by mutating it, nor by overexpressing it, suggesting that its main role is  
483 the regulation of Glass translation.

484

485 In summary, our results suggest that the removal of intron 4, which was added in the  
486 common ancestor of flies and butterflies, is essential for the production of a functional  
487 Glass protein. Stop codon readthrough resulting in an extention of the Glass protein  
488 that is conserved in higher Diptera seems to be dispensable for Glass function in  
489 photoreceptor development. The addition of an exon containing several AUGs  
490 upstream of the Glass start codon found in mosquitoes, can interfere with Glass  
491 translation. Nevertheless, conservation of the upstream start codon and sequence  
492 conservation of the Brs peptide suggest that higher Diptera have found a way to  
493 overcome this interference and that Brs might even have adopted a beneficial  
494 function.

495

496 **MATERIAL AND METHODS**

497

498 **Fly strains**

499

500 Flies were reared at 25°C on a cornmeal medium containing agar, fructose,  
501 molasses, and yeast. Strains for site directed integration (25709, 25710), *w*<sup>1118</sup>  
502 mutants (3605), deficiency lines (4431, 7657) [33], balancer lines (36305, 8379), and  
503 *nos*-Cas9 expressing flies (54591) [34] were obtained from the Bloomington stock  
504 center. *ey-Gal4* expressing flies were a kind gift from R. Stocker.

505

506 **Transgenic constructs**

507 All oligos used for cloning and all sequencing reactions were purchased from  
508 microsynth. The following primer sequences show the annealing sequence part in  
509 capitals and any additional sequence in small letters. Restriction sites are underlined.

510

511 A 5257 basepair long PCR fragment was amplified from genomic DNA of CantonS  
512 flies using primers “glass -4301 Asc fw” (5’-  
513 ggcgcgccTAACCCGATACAAATGGAGAGG-3’) and glass 5’UTR Not re“ (5’-  
514 gcggccgcGACATGACTCCACTTCTGGAAC-3’). The fragment was inserted into  
515 pCR-Blunt II-TOPO vector (Invitrogen). From there it was excised using the  
516 restriction enzymes Ascl and Notl and cloned into a GFP reporter vector (pDVattBR,  
517 kind gift from Jens Rister) to generate the basic *glass*-GFP reporter construct (Fig.  
518 1A, B’). The plasmid was injected into *y, w; attP2* embryos to produce transgenic flies  
519 (Genetic services Inc.).

520

521 To delete the two upstream start codons, a 1483 bp PCR product was amplified from  
522 the original *glass*-GFP reporter plasmid using primers “glass -597 fw” (5’-  
523 TAAAAACTACTGAAAATGCTGCCGATG-3’) and “glass exon2 noAUG Pme re” (5’-  
524 gcgttaaacGATGCGTTAATTCCAATGCAAGGC-3’), TOPO cloned into pCRII,  
525 sequenced, digested Xhol-Pmel, and transferred into the original plasmid also cut  
526 with Xhol-Pmel, thereby removing the 104 basepairs encoding the N-terminus of Brs,  
527 and part of the multiple cloning site of the vector (Fig. 1C’).

528

529 To put the GFP coding sequence in frame with the upstream start codon, the GFP  
530 coding sequence was amplified by PCR using the primers “GFP noStart Not fw” (5’-  
531 tcgcggcccgGGTGAGCAAGGGCGAGG-3’) putting a NotI site in front of GFP  
532 (starting with the 3<sup>rd</sup> nucleotide of GFP) and “GFP down Fse re” (5’-  
533 GATTATGATCTAGAGTCGCGGCCG-3’) covering an FseI and an XbaI site in the  
534 plasmid. The PCR product was cloned NotI-XbaI into pBluescript, sequenced, and  
535 transferred NotI-FseI into the original glass-GFP reporter plasmid deleting most of  
536 the multiple cloning site and the GFP start codon (Fig.1D’).

537

538 For the enhancer analysis, the construct lacking the upstream start codons was  
539 digested with different combinations of restriction enzymes and religated. For  
540 construct B the plasmid was digested with BgIII cutting in the multiple cloning site at  
541 the 5'-end of the enhancer and with BamHI cutting at position -3123. A second  
542 BamHI site at position -1885 was not in the database sequence but is present in the  
543 fragment amplified from the CantonS flies. Therefore, religation of the plasmid after  
544 BgIII-BamHI digestion (the two enzymes producing compatible sticky ends) resulted  
545 in an enhancer fragment ranging from position -1885 to +886. For construct C the  
546 plasmid was digested with EcoRI cutting at the multiple cloning site at the 5'-end of  
547 the enhancer and at positions -1598 and -2040 in the enhancer. Religation resulted  
548 in an enhancer fragment ranging from position -1598 to +886. For construct D the  
549 plasmid was digested with XbaI cutting in the multiple cloning site at the 5'-end of the  
550 enhancer and at position -703. Religation resulted in an enhancer fragment ranging  
551 from -703 to +886. For construct E, construct C was digested with XbaI cutting in the  
552 multiple cloning site at the 5'-end and at position -703 in the enhancer as well as with  
553 Xhol cutting at position -239 in the enhancer. The two ends were filled using Klenow  
554 polymerase and religated resulting in an enhancer fragment ranging from position -  
555 239 to +886. For construct F, construct B was digested with EcoRI cutting at position  
556 -1598 and Xhol cutting at position -239. The two ends were filled using Klenow  
557 polymerase and religated resulting in an enhancer fragment ranging from position -  
558 1885 to -1598 fused to the minimal promoter fragment from position -239 to +886.  
559 For construct G, the original -4301 to +886 plasmid was digested with NheI cutting at  
560 positions -1910, -1903, and -682, the site at position -2179 is missing in our enhancer  
561 fragment amplified from CantonS flies. In another reaction the original plasmid was  
562 digested with EcoRI cutting at positions -1598 and -2040. Both reactions were filled

563 using Klenow polymerase, digested with BgIII, and then the BgIII-NheI<sub>filled</sub> fragment  
564 was ligated into the BgIII-EcoRI<sub>filled</sub> fragment fusing the enhancer region from -4301  
565 to -1910 to the region from -1598 to +886. For construct H, the original plasmid was  
566 digested BamHI-Xhol. The two ends were filled using Klenow polymerase and  
567 religated to fuse the fragment from -4301 to -3123 to the fragment from -239 to +886.  
568 For construct I, the original plasmid was digested with NheI and in an independent  
569 reaction with Xhol. Both digestion reactions were filled with Klenow polymerase. The  
570 NheI<sub>filled</sub> reaction was further digested with BamHI and the Xhol<sub>filled</sub> reaction was  
571 further digested with BgIII. Then the BamHI-NheI<sub>filled</sub> fragment was ligated into the  
572 BgIII-Xhol<sub>filled</sub> plasmid resulting in a fusion of an enhancer fragment ranging from -  
573 3123 to -1910 to the minimal promoter ranging from -239 to +886.  
574 All constructs were injected into *nos-ΦC31;; attP2* flies for site directed integration.  
575 The G0 flies were crossed individually to *w<sup>1118</sup>* flies to screen for *w<sup>+</sup>* offspring. *w<sup>+</sup>* F1  
576 flies were crossed individually to 3<sup>rd</sup> chromosome balancer flies (*w;; Dr e/TM3*) and  
577 their balanced offspring was crossed inter se to produce stable lines.  
578  
579 For the UAS constructs we used the *glass* cDNA plasmid GH20219 as starting point.  
580 This cDNA still contains intron 4 due to incomplete splicing resulting in the RB  
581 transcript isoform. To remove the intron, two PCR reactions were set up. One with  
582 primers “*glass* 5’UTR BamHI fw” (5’-gaggatCCTGCCAAAAGTCGCTTCTT-3’) and  
583 “*glass* exon4 re” (5’-ccccgactgcgaaaatCTGAGCAGGCAGAGCTTGCAC-3’) resulting  
584 in a fragment ranging from the 5’-end of the 5’UTR to the end of exon 4, with the  
585 sequence given in small letters of the reverse primer overlapping with the beginning  
586 of exon 5. The other PCR reaction was done with primers “*glass* exon5 fw” (5’-  
587 gctctgcctgctCAGATTTCGCAGTCGGGAACTT-3’) and “*gl* Stop Xho re” (5’-  
588 ggctcgaGTCATGTGAGCAGGCTTGC-3’), resulting in a fragment ranging from  
589 the beginning of exon 5 to the PA stop codon, with the sequence given in small  
590 letters of the forward primer overlapping with the end of exon 4. Both PCR products  
591 were mixed together to provide the template for another PCR reaction with primers  
592 “*gl* 5’UTR BamHI fw” and “*gl* Stop Xho re”. The resulting PCR product ranging from  
593 the 5’UTR to the PA stop codon without intron 4 was digested with BamHI-Xhol and  
594 cloned into pBluescript. After sequencing, different fragments were PCR amplified.  
595 The Glass PA coding sequence was amplified with primers “*gl* Start+Kozak attB1 fw”  
596 (5’-

597 ggggacaagttgtacaaaaaagcaggctcaaCATGGGATTGTTATAAGGGTCCAACT-  
598 3') and "gl Stop attB2 re" (5'-  
599 ggggaccacttgtacaagaaagctgggtcgTCATGTGAGCAGGCTGTTGCC-3'). The *brs*  
600 sequence was amplified with primers "glass+Smurf attB1 fw" (5'-  
601 ggggacaagttgtacaaaaaagcaggctcCGCATCAAGATGAAGCGTAGGAAAAGC-3') and  
602 "glass Smurf Stop attB2 re" (5'-  
603 ggggaccacttgtacaagaaagctgggtcTCAGGAGTTGGAACCCTTATAACAAATCCC-  
604 3'). The *brs-glass-PA* sequence was amplified with primers "glass+Smurf attB1 fw"  
605 and "gl Stop attB2 re". The primer sequence in small letters are the attB parts used  
606 for gateway cloning. The PCR products were gateway cloned into pENTRY201,  
607 sequences, and transferred into the vector *pUASg.attB* for injection (Genetic  
608 Services Inc.). *UAS-glass-PA* and *UAS-brs-Glass-PA* were injected into *nos-ΦC31;*  
609 *attP40* flies, while the *UAS-brs* plasmid was injected into *nos-ΦC31;; attP2* flies. After  
610 balancing the transgenic flies, *UAS-glass-RA<sup>attP40</sup>* and *UAS-brs<sup>attP2</sup>* were combined in  
611 a single line: *w; UAS-GlassRA<sup>attP40</sup>; UAS-Brs<sup>attP2</sup>*. The different UAS-construct  
612 bearing flies were crossed to *ey-Gal4/CyO* flies, and the number of offspring with *Cy<sup>+</sup>*  
613 versus the number of offspring with *CyO* wings was determined. For calculation of  
614 the survival rate the number of *Cy<sup>+</sup>* flies was divided by the number of *CyO* flies  
615 (Table 1).

616

## 617 CRISPR

618 For the alterations of the endogenous glass locus by CRISPR/Cas9 genome editing,  
619 we assembled the different templates in pBluescript. For the Glass PA+PC variant,  
620 we needed to remove intron 4 from the genomic DNA without changing the sequence  
621 at the Glass PA stop codon. Since there were no useful restriction sites between the  
622 intron 4 / exon 5 junction and the Glass PA stop codon, we decided to introduce an  
623 NdeI site in this sequence by altering a single nucleotide in the third position of the  
624 codon for the first histidine residue of the last zinc-finger (histidine 567 of Glass PA:  
625 CAC to CAT). We PCR amplified a 932 bp fragment from the genomic DNA of *nos-*  
626 *Cas9* flies using primers "glass ex5 R1 Nde fw" (5'-  
627 gagaattcatATGCGCGTCCACGGCAAC-3') and "glass 3'UTR re" (5'-  
628 GATCAAAGCACCTGTCTTACATCTACGTCTAG-3'), and a 1529 bp fragment from  
629 the intronless glass version assembled in pBluescript for generation of the *UAS-*  
630 *glass-PA* construct using primers "glass ex4 R1 fw" (5'-

631 cggaattCAAGAGTGCGCCGCTTCC-3') and "glass ex5 Nde re" (5'-  
632 CGCATaTGCCGATTCAAGTTCCCCGAC-3'). Both PCR products were combined in  
633 pBluescript vector by digesting the one covering the C-terminus from the Ndel site  
634 introduced in exon 5 to an endogenous HindIII site in the 5'UTR with Ndel-HindIII,  
635 and the one covering exon 4 and part of exon 5 with EcoRI-Ndel (due to an  
636 endogenous Ndel site in the middle of exon4 this part was cloned in two steps). The  
637 sequence of the resulting fragment ranging from the beginning of exon 4 to the  
638 5'UTR and lacking intron 4 was confirmed.

639

640 For the Glass PB variant, we introduced a deletion ranging from the end of intron 4 to  
641 the middle of the sequence added in the extended Glass PC protein version (Fig. 4A).  
642 We amplified two PCR products from the genomic DNA of *nos*-Cas9 flies. A 1866 bp  
643 fragment spanning exon 4 and most of intron 4 was amplified with primers "glass ex4  
644 R1 fw" and "glass int4 Xho re" (5'-AACTCGAgGTATAACGTTCCAGGACTGCTC-3'),  
645 and a 1287 bp fragment ranging from the middle of the Glass PC encoding sequence  
646 to a place located around 5000 bp downstream of the *glass* gene was amplified with  
647 primers "glass 3'UTR Xho fw" (5'-aactcgAGCATCGGCGATTATACTCCACC-3') and  
648 "glass down Kpn re" (5'-agggtACCTTTTGGTGGCCTCCCAGG-3'). Both fragments  
649 were subcloned, sequenced and combined in pBluescript by digesting the one  
650 covering exon 4 and intron 4 with EcoRI-Xhol, and the one covering part of the PC  
651 coding region, the 3'UTR and downnstream genomic sequence with Xhol-Acc65I.

652 For the Glass PA+PB variant, we introduced two additional stop codons at the end of  
653 the Glass PA encoding part and deleted 29 of the nucleotides following the stop  
654 codon. We PCR amplified two PCR products from the genomic DNA of *nos*-Cas9  
655 flies. A 2034 bp fragment spanning exon 4, intron 4, and the PA encoding part of  
656 exon 5 was amplified with primers "glass ex4 fw" and "glass RA **3xStop** Xho re" (5'-  
657 ctctcgag**ctatta**TCATGTGAGCAGGCTTGCAC-3'). A 1365 bp fragment spanning  
658 most of the Glass RC specific sequence, the 3'UTR and around 500 nucleotides of  
659 downstream genomic sequence was amplified using primers "glass RC Xho fw" (5'-  
660 ttctcgAGCATTACCACCCCCCGC-3') and "glass down Kpn re". Both fragments were  
661 subcloned, sequenced, and combined in pBluescript by digesting the one covering  
662 exon 4, intron 4, and the Glass PA encoding part plus stop codons with EcoRI-Xhol,  
663 and the one covering the Glass PC region, 3'UTR, and downstream genomic  
664 sequence Xhol-Acc65I.

665

666 For the Glass PA variant, we performed a PCR amplification of exon 4 and the 5'-end  
667 of exon 5 with the same first primer pair as for the Glass PA+PB template, but using  
668 the intronless glass version assembled in pBluescript for generation of the *UAS-*  
669 *glass-PA* construct as a template. We subcloned this 1638 bp fragment EcoRI-Xhol,  
670 sequenced it, and combined it with the 1365 bp fragment spanning most of the Glass  
671 RC specific sequence, the 3'UTR and around 500 nucleotides of downstream  
672 genomic sequence.

673

674 For expression of the CRISPR guideRNAs, sense and antisense oligos with  
675 overhangs fitting the sticky ends of the BbsI digested vector were annealed and  
676 ligated into pU6-BbsI-chiRNA plasmid (a gift from Melissa Harrison & Kate O'Connor-  
677 Giles & Jill Wildonger, Addgene plasmid # 45946 [35]). Site 1  
678 (ctgctcagggtgagtccg/gga) is located at the junction between exon 4 and intron 4. Site 2  
679 (gtcccacagatttcgca/gtc) is located at the junction between intron 4 and exon 5. Site 3  
680 (agg/agtgccaggaggttcca) guides Cas9 to cut 12 bp downstream of the Glass PA stop  
681 codon. Site 4 (aca/tggtaactacgactac) is located in the middle of the Glass PC  
682 encoding region (Fig. 4A). CRISPR sites were selected based on their position in the  
683 glass genomic sequence using a CRISPR site prediction program  
684 (<http://tools.flycrispr.molbio.wisc.edu/targetFinder/> [36]).

685

686 The templates for the different Glass isoform variants were co-injected with sgRNA  
687 expression plasmids into embryos of *nos-Cas9* flies. The Glass PA+PC variant was  
688 co-injected with the sgRNA plasmids for sites 1 and 2. The template for the Glass PB  
689 variant was co-injected with sgRNA plasmids for sites 2 and 4. The template for the  
690 Glass PA+PB variant was co-injected with the sgRNA plasmid for site 3. The template for the  
691 Glass PA variant was co-injected with the sgRNA plasmids for sites  
692 1 and 3. The resulting G0 flies were crossed individually with deficiency lines  
693 uncovering the *glass* locus. Some of the offspring resulting from Cas9 cutting at  
694 CRISPR site 1 (and 3) showed a *glass* mutant phenotype due to CRISPR induced  
695 non homologous end joining (Fig. S5). Irrespective of the eye phenotype the offspring  
696 was crossed individually with third chromosome balancer flies (*w*; *Dr*, *e/TM3*) and  
697 analyzed by PCR for the introduced deletions and sequence alterations. The *glass*  
698 genes of those lines that showed changes in the PCR analyses, were sequenced to

699 confirm the introduced changes and identify other alterations that resulted in *glass*  
700 mutant phenotypes.

701

702 For the deletions in the *brs* sequence, template sequences were assembled in  
703 pBluescript. For the 1nt deletion two PCR products were amplified. A 2759 bp  
704 fragment ranging from position -1863 in the glass enhancer region to position +896 in  
705 the *brs* coding sequence was amplified using primers “glass -2700 Kpn fw” (5'-  
706 tgggtacCGGCAGCAGAGACAGGGCTC-3') and “smurf -1nt H3 re” (5'-  
707 ccaaGCTTCATCTTGATGCGTTAATTCCAAGTGC-3'). The resulting PCR product  
708 was cloned Acc65I-HindIII into pBluescript and sequenced. A 2493 bp fragment  
709 ranging from position +899 in the *brs* coding sequence to position +3392 at the end  
710 of exon 4 was amplified from *nos*-Cas9 genomic DNA using primers “smurf -1nt H3  
711 fw” (5'-gaaagcttGGAAAAGCAGGAACAAATGCGCG-3') and “glass exon4 Pst re” (5'-  
712 ctctGCAGGCAGAGCTTGCAGTGG-3'). The resulting PCR product was cloned  
713 HindIII-PstI into pBluescript, sequenced, and combined with the 5'-fragment. For the  
714 5 nt deletion fusing Brs with Glass, A 2821 bp fragment ranging from position -1863  
715 to +953 in the *brs* coding sequence just before the second AUG codon was amplified  
716 from *nos*-Cas9 genomic DNA using primers “glass -2700 Kpn fw” and “smurf -5nt  
717 BamH Nco re” (5'-ccggatccCATGgCTCCACTTCTGGAACGTTGGGC-3'). The  
718 resulting PCR product was cloned Acc65I-BamHI into pBluescript and sequenced. A  
719 1632 bp fragment ranging from position +959 just before the Glass start codon to  
720 position +2591 in exon 4 was amplified from *nos*-Cas9 genomic DNA using primers  
721 “smurf -5nt Nco fw” (5'-ctcCATGGGATTGTTATATAAGGGTCCAAACTCCTG-3')  
722 and “glass ex4 Not re” (5'-aagcggccgcatggcatggcatgtcatgc-3'), cloned Ncol<sub>filled</sub>-  
723 NotI into pBluescript BamHI<sub>filled</sub>-NotI, sequenced, and combined KpnI-Ncol with the  
724 5'-fragment. For expression of the CRISPR guideRNAs, sense and antisense oligos  
725 with overhangs fitting the sticky ends of the BbsI digested vector were annealed and  
726 ligated into the BbsI digested pCDF4-U6:1\_U6:3tandemgRNAs plasmid (gift from  
727 Simon Bullock, addgene plasmid # 49411). The site for the -1nt deletion  
728 (aacgcatcaagatgaag/cgt) is located at the upstream start codon, the site for the -5nt  
729 deletion (ccagaagtggagtcatg/tca) is located at the Glass start codon (Fig. 3A). The  
730 templates for the *brs* mutations were co-injected with the corresponding sgRNA  
731 expression plasmid into embryos of *nos*-Cas9 flies. The resulting G0 flies were  
732 crossed individually with deficiency lines uncovering the glass locus. Some of the F1

733 flies had a very subtle rough eye phenotype over the glass deficiency – but also over  
734 the TM6b balancer. The F1 flies were crossed individually with 3<sup>rd</sup> chromosome  
735 balancer flies to establish stocks, and tested by PCR and restriction digest with either  
736 HindIII or Ncol for presence of the introduced changes. Genomic DNA of the *glass*  
737 locus from homozygous candidates was PCR amplified and sent for sequencing.  
738 Additional sequence changes due to non-homologous end joining were also  
739 identified (Fig. S3).

740  
741

#### 742 **Light Preference Assay**

743 The light preference assays were prepared and performed under red light conditions  
744 during the subjective day. *Drosophila melanogaster* adults of both sexes were used.  
745 Given that light perception in *Drosophila* is affected by age [6], for consistency, we  
746 used <1 day old flies in all our experiments. Without anaesthesia 20 – 40 flies were  
747 taken from food vials and loaded into the elevator chamber of a T-maze. The elevator  
748 chamber was descended and flies were allowed to move freely between the elevator  
749 chamber and two plastic tubes for 2 min. A white LED was placed at one end of one  
750 testing tube. Thus, only one testing tube was illuminated. After 2 min the elevator  
751 chamber was ascended and flies were not able to move between testing tubes and  
752 elevator chamber. We determined the number of flies in the illuminated testing tube  
753 (L) and the number of flies in the dark testing tube (D) as well as the number of flies  
754 in the elevator chamber (E). We calculated a preference index as follows:

755

756 Light intensity was measured from the distance of the elevator chamber to the LED.  
757 The light intensity was 1338  $\mu\text{W}/\text{cm}^2$  with a first maximum intensity peak of 16.6  
758  $\mu\text{W}/\text{cm}^2/\text{nm}$  at 443 nm with half-widths of around 11 nm and a second maximum  
759 intensity peak of 6.8  $\mu\text{W}/\text{cm}^2/\text{nm}$  at 545 nm with half-widths of around 62 nm.

760

#### 761 **Electroretinogram**

762

763 ERG recordings were obtained as previously described [37]. Briefly, we mounted  
764 living flies inside a pipette tip, leaving their heads outside, and immobilised them with  
765 a mixture of bee wax and colophony 3:1, which worked as a glue. We placed the flies  
766 inside a dark chamber and applied two electrodes: a ground electrode was  
767 positioned inside the head of the fly, and a recording electrode was introduced into

768 the retina. In our stimulation protocol, we illuminated the compound eye with orange  
769 light for 5 seconds to transform all metarhodopsin to rhodopsin, switched off the light  
770 for 10 seconds, and illuminated again a second time with orange light for another 5  
771 seconds. We recorded the response of PRs to the second stimulus.

772

### 773 **Immunohistochemistry**

774

775 Eye imaginal discs were dissected from third instar larvae and fixed in 3.7%  
776 formaldehyde dissolved in phosphate buffer (PB) for 20 minutes.

777

778 For cryosections, we dissected the heads of the flies and fixed them for 20 minutes  
779 with 3.7% formaldehyde dissolved PB, as previously described [1]. We washed these  
780 samples by using phosphate buffer with Triton 0.3% (PBT) and incubated them  
781 overnight in cryoprotected solution (25% sucrose in PB). Then, we embedded the  
782 heads in OCT, froze them, and took 14  $\mu$ m sections by using a cryostat.

783

784 Both eye imaginal discs and cryosections were washed with PBT, and incubated  
785 sequentially in primary and secondary antibodies (each antibody incubation step was  
786 performed overnight, washing with PBT between and in the end of these steps). We  
787 used Vectashield as a mounting medium.

788

789 As primary antibodies, we used rabbit anti-GFP (1:1000, Molecular probes, A-6455),  
790 and guinea pig anti-Sens (1:800, courtesy of H. Bellen [38]). To stain against  
791 phototransduction proteins we used antibodies generated in C. Zuker's lab: anti-  
792 NorpA (1:100), rabbit anti-Trpl (1:100), both of which were kindly provided by N.  
793 Colley. The following antibodies were obtained from Developmental Studies  
794 Hybridoma Bank (DSHB) at The University of Iowa: mouse anti-Rh1 (1:20, 4C5),  
795 mouse anti-Trp (1:20, MA83F6), and rat anti-Elav (1:30, No. 7E8A10)

796

797 Secondary antibodies were obtained from Molecular probes, and we used the  
798 conjugated with the following Alexa fluor proteins: 488, 568, and 647. In addition, we  
799 also used Hoechst 33258 (1:100, Sigma, No. 94403)

800

### 801 **ACKNOWLEDGEMENTS**

802  
803 We thank J. Rister and S. Bullock for plasmids; M. Harrison, K. O'Connor-Giles, and  
804 J. Wildonger for the pU6-BbsI-gRNA plasmid and the CRISPR target finder website;  
805 R. Stocker for the *ey-Gal4* flies; and N. Colley, H. Bellen, and the DSHB for  
806 antibodies. We thank J. E. Treisman for helpful comments and discussions. We are  
807 also grateful to our colleagues from the Sprecher and Huber labs for valuable  
808 discussions, particularly thanks to B. Egger, T. Smylla and O. Voolstra. This work  
809 was supported by the Swiss National Science Foundation (grant number  
810 31003A\_149499), the Novartis Foundation for Biomedical Research (grant number  
811 18A017) and the University of Fribourg to S.G.S.

812  
813

814 **Figure Legends**

815 **Figure 1: *glass* reporter constructs.** A: genomic region of *glass* including the 5.2  
816 kb regulatory region (yellow), the three *glass* isoforms (RA, RB, RC) with their intro-  
817 exon structures, stop codons (asterisks), the protein coding regions (purple), and the  
818 positions of the five zinc fingers (magenta). The position of the upstream overlapping  
819 open reading frame (smORF) is indicated in blue. A non-coding RNA (orange) is  
820 located upstream of the *glass* gene. The 5.2 kb upstream genomic region including  
821 the non coding exon 1 and the 5'end of exon 2 were cloned in front of eGFP (green).  
822 B: eye imaginal disc of a fly transgenic for the *glass*-GFP reporter construct (-4301 to  
823 +959). The GFP expression level is very low. B': sequence fragment of the *glass*-  
824 GFP reporter construct including the 5'end of exon 2, the linker, and the first two  
825 codons of GFP (MV). The positions of the two upstream start codons and the GFP  
826 start codon are indicated by arrows. Translation from the upstream start codon  
827 results in the production of a protein encoded by the 3<sup>rd</sup> reading frame of eGFP (first  
828 44 amino acids shown in blue box). B'': GFP channel alone of the disc shown in  
829 panel B. No GFP is detectable (gain: 621.7). B'': close up of the region indicated by  
830 the white box in B. B'''': GFP channel alone of the region outlined in panel B imaged  
831 with a higher gain (827.1). GFP levels are slightly higher in the posterior region of the  
832 discs. C: eye disc of a transgenic fly expressing a *glass*-GFP reporter construct in  
833 which the two upstream start codons were deleted. GFP is expressed at high level in  
834 the posterior region of the disc that will give rise to the adult eye. C': Sequence

835 fragment of the GFP reporter construct indicating the part that was excised to remove  
836 the upstream start codons (-4301 to +886). Translation can only start at the GFP start  
837 codon. C'': GFP channel alone of the disc shown in panel C (gain: 621.7). C'''': close  
838 up of the region indicated by the white box in C. C''''': GFP channel alone of the  
839 region outlined in panel C (gain 621.7). eGFP is mainly cytoplasmic. D: eye disc of a  
840 transgenic fly expressing a *glass*-GFP reporter construct in which the GFP start  
841 codon was deleted and the GFP coding sequence is in frame with the upstream start  
842 codon(s). D' Sequence fragment of the GFP reporter construct indicating the part that  
843 was excised to remove the GFP start codon (-4301 to +959 in frame). The N-  
844 terminus of the resulting fusion protein between the upstream translation product and  
845 GFP is shown below). D'': GFP channel alone of the disc shown in panel D (gain:  
846 757.2). D''': close up of the region indicated by the white box in D. D''''': GFP channel  
847 alone of the region outlined in panle D (gain 757.2). GFP shows nuclear localization.  
848 All discs are oriented with the posterior to the right. Discs were stained with  
849 antibodies against GFP (green), Elav (red), FasIII (blue in panels B'', C'' and D''')  
850 and with DAPI (blue in panels B, C and D). Scale bars in panels B, B'', C, C'', D and  
851 D'' are 50  $\mu$ m, in panels B'', B''', C''', C''''', D'' and D'''' are 20  $\mu$ m long.  
852

853 **Figure 2: Functional analysis of the *glass* enhancer region.** A: enhancer  
854 fragments used to drive GFP expression. The construct with the deleted upstream  
855 start codons (top) was fragmented using the restriction sites indicated above. The  
856 resulting reporter constructs are shown below. B-I: GFP expression patterns of  
857 constructs B to I. All discs are oriented with the posterior end to the right. Scale bas:  
858 50 $\mu$ m. Arrows: ocelli anlage. B'-I': close ups of the regions marked by the rectangles  
859 in panel B to I. Scale bars: 20  $\mu$ m. Arrow head: GFP expression anterior of the  
860 morphogenetic furrow. Discs were stained with antibodies against GFP (green), Elav  
861 (red), FasIII (blue in panels B' to I'), and with DAPI (blue in panels B-I)  
862  
863

864 **Figure 3: The upstream overlapping open reading frame is not required for eye  
865 development or function.** A: sequence of *glass* exon 2. The positions of the  
866 upstream start codon (+889) and the Glass start codon (+960) are indicated by  
867 arrows. CRISPR sites are underlined in red, and the actual positions of the cuts are  
868 indicated by a vertical red line. The amino acid sequence of the Glass N-terminus is

written in the blue box under the coding sequence. The *brs* nucleotide and amino acid sequence is shown in the orange box. A single nucleotide deletion was introduced in the *brs*<sup>-1nt</sup> allele (followed by an A to T mutation to generate a HindIII restriction site). This will result in a frameshift completely changing the amino acid sequence of the Brs peptide (shown in the green box) with only a minimal change in the nucleotide sequence of exon 2. The resulting peptide still overlaps with the Glass open reading frame. A 5 nucleotide deletion was introduced in the *brs*<sup>-5nt:Glass</sup> allele between the second Brs AUG and the second codon of Glass, putting both sequences into the same frame as indicated by the orange and blue underlaid sequences (a T to C mutation was introduced to generate an Ncol site, changing the valine at position 22 of this fusion protein into alanine). B: adult eye, expression of the retinal markers Rh1, NorpA, Trp, and Trpl and ERG of control *w*<sup>1118</sup> flies. C: adult eye, expression of the retinal markers Rh1, NorpA, Trp, and Trpl and ERG of *brs*<sup>-1nt</sup> deletion flies. D: adult eye, expression of the retinal markers Rh1, NorpA, Trp, and Trpl and ERG of *brs*<sup>-5nt:Glass</sup> deletion flies. B-D: All antibody stainings are shown in green, DNA was stained with Hoechst (purple). Scale bars represent 40  $\mu$ m. Flies of all tested genotypes are attracted by light. Two-tailed one sample *t* test followed by the Benjamini Hochberg procedure: For all data sets  $n = 7$  experiments. CTRL:  $p = 3.6 \times 10^{-8}$ ,  $t_{(6)} = 31.09$ ; *brs*<sup>-1nt</sup>:  $p = 1 \times 10^{-5}$ ,  $t_{(6)} = 13.88$ ; *brs*<sup>-5nt:Glass</sup>:  $p = 1.1 \times 10^{-5}$ ,  $t_{(6)} = 13.38$ . The light preference index of all experimental groups is not different from the light preference index of the control group. One-way ANOVA of preference indices:  $p = 0.495$ ,  $F\text{-Value}_{(5,36)} = 0.895$ . Data show mean and error bars show standard deviation. Red dots indicate means of individual experiments. E-H: overexpression of UAS constructs with a strong ey-Gal4 driver. E: Overexpression of the Glass PA protein leads to severe eye and head defects resulting in pharate lethality. F: the only ey-Gal4>UAS-Glass-PA fly that eclosed had very small eyes. G: Overexpression of the Brs peptide did not affect eye or head development. H: When expressed together on the same UAS-construct, Brs translation interferes with Glass translation resulting in a higher number of escapers that have small or even normal eyes.

898

899 **Figure 3: Isoform specific *glass* alleles.** A: wildtype and mutated versions of *glass*  
900 from the end of exon 4 to the end of the transcript. Stop codons of isoforms PA, PB,  
901 and PC are indicated by asterisks. The C2H2-zinc-finger region is shown in purple  
902 and magenta. Intron 4 is shown in white. The C-terminus of the PA isoform is shown

903 in blue, that of the PC isoform in yellow. The 3'UTR is grey. The positions of the  
904 CRISPR sites used for mutagenesis are shown as green boxes. Deletions are  
905 indicated as black lines. The triple stop codon introduced in the PA+PB and the PA  
906 alleles are indicated by red boxes and asterisks. B: adult eye and expression of the  
907 retinal markers Rh1, NorpA, Trp, and Trpl in control  $w^{1118}$  flies as indicated above. C:  
908 adult eye and expression of the retinal markers Rh1, NorpA, Trp, and Trpl in flies  
909 expressing the Glass PA +PC isoforms. D: adult eye phenotype and loss of  
910 expression of the retinal markers Rh1, NorpA, Trp, and Trpl in flies expressing the  
911 Glass PB isoform. E: adult eye and expression of the retinal markers Rh1, NorpA,  
912 Trp, and Trpl in flies expressing the Glass PA +PB isoforms. F: adult eye and  
913 expression of the retinal markers Rh1, NorpA, Trp, and Trpl in flies expressing the  
914 Glass PA isoform. B-F: All tested markers are expressed in the different alleles,  
915 except in the mutant only expressing the PB isoform, which has a *glass* mutant eye  
916 phenotype. All antibody stainings are shown in green, DNA was stained with Hoechst  
917 (magenta). Scale bars represent 40  $\mu$ m G: ERGs of the different *glass* isoform alleles  
918 indicated at the left, scale bars represent 5 mV (vertical) and 5 seconds (horizontal).  
919 H: Light preference index of wildtype and flies that are mutant for specific Glass  
920 isoforms. Flies expressing only the PB isoform are photoneutral. Two-tailed one  
921 sample *t* test followed by the Benjamini Hochberg procedure: For all data sets  $n = 10$   
922 experiments. CTRL:  $p = 5.8 \times 10^{-9}$ ,  $t_{(9)} = 23.82$ ; PA+PC:  $p = 2.1 \times 10^{-9}$ ,  $t_{(9)} = 30.20$ ; PB:  
923  $p = 0.46$ ,  $t_{(9)} = 0.97$ ; PA+PB:  $p = 6.6 \times 10^{-7}$ ,  $t_{(9)} = 13.43$ ; PA:  $p = 3.8 \times 10^{-9}$ ,  $t_{(9)} = 26.19$ .  
924 Only flies expressing just the Glass PB isoform show a light preference which is  
925 different from the one of control flies. One-way ANOVA of preference indices: For all  
926 data sets  $n = 10$  experiments,  $p < 2 \times 10^{-16}$ ,  $F\text{-Value}_{(8,81)} = 44.04$ . CTRL vs PA+PC:  $p = 1$ ,  
927  $t = -0.15$ ; CTRL vs PB:  $p < 0.001$ ,  $t = 8.11$ ; CTRL vs PA+PB:  $p = 0.23$ ,  $t = 2.03$ ; CTRL  
928 vs PA:  $p = 1$ ,  $t = -0.10$ . Data show mean and error bars show standard deviation. Red  
929 dots indicate means of individual experiments. \*\*\* =  $p < 0.001$ .

930  
931 **Figure S1: *glass*-GFP reporter gene expression patterns.** GFP (green),  
932 Senseless (Sens, red), and Elav (blue) expression in the eye region of larval imaginal  
933 discs of transgenic flies expressing construct C (-1598 to +886) (A), construct F (-  
934 1885 to -1598 / -239 to +886) (B), construct H (-4301 to -3123 / -239 to +886) (C), or  
935 construct I (-3123 to -1906 / -239 to +886) (D) (compare to Fig. 2A for the individual

936 constructs). Scale barr: 40  $\mu$ m A' to D': magnification of areas in panels A to D. Scale  
937 barr: 5  $\mu$ m. A" to D": GFP channel alone.

938

939 **Figure S2: sequence conservation upstream of the glass start codon.** A:  
940 nucleotide sequence of glass exon 2 of different higher *Diptera*. The position of the  
941 glass start codon is outlined in green. The position of the upstream start codon is  
942 outlined in blue. The black vertical lines show the triplets following the upstream  
943 start codon that result in the amino acid sequences shown in B. B: Alignment of the  
944 amino acid sequence resulting from translation beginning at the start codon upstream  
945 of Glass from different higher Diptera. *Drosophila melanogaster* (*D mel*), *Drosophila*  
946 *sechellia* (*D sec*), *Drosophila simulans* (*D sim*), *Drosophila erecta* (*D ere*), *Drosophila*  
947 *yakuba* (*D yak*), *Drosophila takahashii* (*D tak*), *Drosophila eugracilis* (*D eug*),  
948 *Drosophila rhopaloa* (*D rho*), *Drosophila ficusphila* (*D fic*), *Drosophila elegans* (*D ele*),  
949 *Drosophila ananassae* (*D ana*), *Drosophila persimilis* (*D per*), *Drosophila*  
950 *pseudoobscura* (*D pse*), *Drosophila grimshawi* (*D gri*), *Drosophila virilis* (*D vir*),  
951 *Drosophila mojavensis* (*D moj*), *Drosophila willistoni* (*D wil*), *Lucilia cuprina* (*L cup*),  
952 *Musca domestica* (*M dom*), *Glossina morsitans* (*G mor*).  
953

954

955 **Figure S3: *trs* alleles generated by small CRISPR deletions in the *glass* 5'UTR.**  
956 A: sequence alignment of the different *trs* alleles. The *glass* start codon is outlined in  
957 green, the upstream start codon in blue. The second AUG codon in the same frame  
958 as the upstream start codon is outlined in orange. Stop codons relative to the  
959 upstream start codon(s) are outlined in red. B: Adult eye phenotype and expression  
960 of the retinal markers Rh1, NorpA, Trp, and Trpl of *trs*<sup>-2nt</sup> flies. C: Adult eye  
961 phenotype and expression of the retinal markers Rh1, NorpA, Trp, and Trpl of *trs*<sup>-4nt</sup>  
962 flies. D: Adult eye phenotype and expression of the retinal markers Rh1, NorpA, Trp,  
963 and Trpl of *trs*<sup>-5nt</sup> flies. B-D: All antibody stainings are shown in green,  
964 counterstaining of DNA with Hoechst (magenta). All tested photoreceptors are  
965 expressed in the *trs* frameshift alleles. Scale bars: 40  $\mu$ m E: ERGs; scale bars: 5  
966 mV (vertical) and 5 seconds (horizontal). F: Flies of all tested genotypes are attracted  
967 by light. Two-tailed one sample *t* test followed by the Benjamini Hochberg procedure:  
968 For all data sets n = 7 experiments. *trs*-2nt:  $p = 3.6 \times 10^{-8}$ ,  $t_{(6)} = 47.23$ ; *trs*-4nt:  $p =$   
969  $8.9 \times 10^{-6}$ ,  $t_{(6)} = 14.81$ ; *trs*-5nt:  $p = 2 \times 10^{-6}$ ,  $t_{(6)} = 19.97$ . The light preference index of all  
969 experimental groups is not different from the light preference index of the control

970 group. One-way ANOVA of preference indices:  $p = 0.495$ ,  $F\text{-Value}_{(5,36)} = 0.895$ . Data  
971 show mean and error bars show standard deviation. Red dots indicate means of  
972 individual experiments.

973

974 **Figure S4: sequence conservation of intron 4 and Glass PC.** A: nucleotide  
975 sequence of the transition between exon 4 and intron 4 and between intron 4 and  
976 exon 5 of *Drosophila melanogaster*. Other Diptera and Lepidoptera also contain this  
977 intron followed by a stop codon black box) immediately after the exon intron junction  
978 (black line), except in *Heliconius*, where the stop codon is located 17 pb downstream  
979 of the exon intron junction. Although the intron is absent in other insect species, the  
980 amino acid sequence flanking the intron and forming part of the Glass zinc-finger is  
981 highly conserved as indicated by the translation below the alignment. B: amino acid  
982 alignment of the Glass C-termini of different higher Diptera. The position of the Glass  
983 PA stop codon is marked by an asterisk (arrow). The amino acid sequence directly  
984 following the end of the PA isoform is highly conserved. There is also high sequence  
985 conservation at the C-terminus of the PC isoform. The central region, which is rich in  
986 histidine residues, is more variable. *Drosophila melanogaster* (*D mel*), *Drosophila*  
987 *simulans* (*D sim*), *Drosophila sechellia* (*D sec*), *Drosophila erecta* (*D ere*), *Drosophila*  
988 *yakuba* (*D yak*), *Drosophila ananassae* (*D ana*), *Drosophila pseudoobscura* (*D pse*),  
989 *Drosophila persimilis* (*D per*), *Drosophila willistoni* (*D wil*), *Drosophila virilis* (*D vir*),  
990 *Drosophila mojavensis* (*D moj*), *Drosophila grimshawi* (*D gri*), *Musca domestica* (*M*  
991 *dom*), *Glossina morsitans* (*G mor*), *Lucilia cuprina* (*L cup*), *Anopheles darlingi* (*A dar*),  
992 *Anopheles gambiae* (*A gam*), *Culex quinquefasciatus* (*C qui*), *Culex pipiens* (*C pip*),  
993 *Danaus plexippus* (*D ple*), *Heliconius melpomene* (*H mel*), *Apis mellifera* (*A mel*),  
994 *Bombus impatiens* (*B imp*), *Nasonia vitripennis* (*N vit*), *Tribolium castaneum* (*T cas*),  
995 *Pediculus humanus* (*P hum*), *Acyrthosiphon pisum* (*A pim*), *Ixodes scapularis* (*I sca*),  
996 *Drosophila ficusphila* (*D fic*), *Drosophila eugracilis* (*D eug*), *Drosophila biarmipes* (*D*  
997 *bia*), *Drosophila takahashii* (*D tak*), *Drosophila elegans* (*D ele*), *Drosophila*  
998 *bipectinata* (*D bip*), *Drosophila kikkawai* (*D kik*).

999

1000 **Figure S5: Additional *glass* alleles generated by non-homologous end joining.**  
1001 A: wildtype and mutated versions of *glass* from the end of exon 4 to the end of the  
1002 transcript. Stop codons of isoforms PA, PB, and PC are indicated by asterisks. The  
1003 C2H2-zinc-finger region is shown in magenta. Intron 4 is shown in white. The C-

1004 terminus of the PA isoform is shown in blue, that of the PC isoform in yellow. The  
1005 3'UTR is grey. The sequences at the exon intron and intron exon junctions are given  
1006 as letters with a black vertical line depicting the position of the junction. The stop  
1007 codon at the beginning of exon 4 is highlighted in blue. The positions of the CRISPR  
1008 sites used for mutagenesis are underlined in green. Deletions are indicated as black  
1009 lines in the schemes, and as red letters in the sequences. Due to the deletions of the  
1010 exon intron junction and the stop codons, additional amino acids are added to the  
1011 Glass PB sequence until they reach the next stop codon in intron 4 (purple boxes).  
1012 Due to the frameshift caused by the single nucleotide deletion in exon 5, the amino  
1013 acid sequence of the Glass PA isoform gets shifted in  $gl^{del21.3}$  (orange box). B: Adult  
1014 eye phenotype and expression of the retinal markers Rh1, NorpA, Trp, and Trpl of  
1015 the  $gl^{del1.1}$  mutant. C: Adult eye phenotype and expression of the retinal markers Rh1,  
1016 NorpA, Trp, and Trpl of the  $gl^{del22.4}$  mutant. D: Adult eye phenotype and expression of  
1017 the retinal markers Rh1, NorpA, Trp, and Trpl of the  $gl^{del31.9}$  mutant. E: Adult eye  
1018 phenotype and expression of the retinal markers Rh1, NorpA, Trp, and Trpl of the  
1019  $gl^{del21.3}$  mutant. C-E: All antibody stainings are shown in green, counterstaining of  
1020 DNA with Hoechst (magenta). None of the tested photoreceptor makers is expressed  
1021 in these glass alleles. Scale bars: 40  $\mu$ m F: ERGs of the different deletion alleles  
1022 show no response to light, scale bars represent 5 mV (vertical) and 5 seconds  
1023 (horizontal). G: Flies homozygous for the different small deletions in the *glass* locus  
1024 are photoneutral. Two-tailed one sample *t* test followed by the Benjamini Hochberg  
1025 procedure: For all data sets n = 10 experiments.  $gl^{del1.1}$ :  $p = 0.90$ ,  $t_{(9)} = 0.13$ ;  $gl^{del21.3}$ :  $p$   
1026 = 0.53,  $t_{(9)} = -1.11$ ;  $gl^{del22.4}$ :  $p = 0.49$ ,  $t_{(9)} = -1.03$ ;  $gl^{del31.9}$ :  $p = 0.66$ ,  $t_{(9)} = -0.57$ . The  
1027 light preference index of all experimental groups is different from the light preference  
1028 index of the control group shown in Figure 3. One-way ANOVA of preference indices:  
1029 For all data sets n = 10 experiments,  $p < 2 \times 10^{-16}$ ,  $F\text{-Value}_{(8,81)} = 44.04$ . CTRL vs  $gl^{del1.1}$ :  
1030  $p < 0.001$ ,  $t = 8.74$ ; CTRL vs  $gl^{del21.3}$ :  $p < 0.001$ ,  $t = 9.81$ ; CTRL vs  $gl^{del22.4}$ :  $p < 0.001$ ,  $t$   
1031 = 10.12; CTRL vs  $gl^{del31.9}$ :  $p < 0.001$ ,  $t = 9.20$ . Data show mean and error bars show  
1032 standard deviation. Red dots indicate means of individual experiments. ns = not  
1033 significant.

1034

1035

1036

1037 **REFERENCES**

1038

1039 1. Bernardo-Garcia FJ, C. Fritsch, S.G. Sprecher. The transcription factor Glass links eye  
1040 field specification with photoreceptor differentiation in *Drosophila*. *Development*. 2016  
1041 143:1413-23. doi: 10.1242/dev.128801.

1042 2. Liang X, Mahato, S., Hemmerich, C., Zelhof, A.C. Two temporal functions of Glass:  
1043 Ommatidium patterning and photoreceptor differentiation. *Dev Biol*. 2016;414(1):4-20. doi:  
1044 10.1016/j.ydbio. PubMed Central PMCID: PMCPMC4875859.

1045 3. Moses K, Ellis, M.C., Rubin, G.M. The glass gene encodes a zinc-finger protein  
1046 required by *Drosophila* photoreceptor cells. *Nature*. 1989;340:531-6.

1047 4. Morrison CA, Chen, H., Cook, T., Brown, S., Treisman, J.E. Glass promotes the  
1048 differentiation of neuronal and non-neuronal cell types in the *Drosophila* eye. *PLoS Genet*.  
1049 2018;2018(14):1. doi: 1371/journal.pgen.1007173. PubMed Central PMCID:  
1050 PMCPMC5783423.

1051 5. Bridges CB, Morgan, T.H. The third-chromosome group of mutant characters of  
1052 *Drosophila melanogaster*. Washington: Carnegie Institution of Washington1923; 1923.

1053 6. Bernardo-Garcia FJ, Humberg, T.H., Fritsch, C., Sprecher, S.G. Successive  
1054 requirement of Glass and Hazy for photoreceprot specification and maintenance in *Drosophila*.  
1055 *Fly (Austin)*. 2017;11(2):112-20. doi: 10.1080/19336934.2016.1244591. PubMed Central  
1056 PMCID: PMCPMC5406162.

1057 7. Moses K, Rubin, G.M. glass encodes a site-specific DNA-binding protein that is  
1058 regulated in response to positional signals in the developing *Drosophila* eye. *Genes &*  
1059 *Development*. 1991;5(4):583-93.

1060 8. Liu H. MC, Moses K. Identification and functional characterization of conserved  
1061 promoter elements from glass: a retinal development gene of *Drosophila*. *Mech Dev*.  
1062 1996;56(1-2):73-82.

1063 9. Kosugi s, Haseve, M., Tomita, M., Yanagawa, H. Systematic identification of yeast  
1064 cell cycle-dependent nucleocytoplasmic shuttling proteins by prediction of composite motifs.  
1065 *Proc Natl Acad Sci USA*. 2009;106(10171-10176).

1066 10. Ready DF, Hanson, T.E., Benzer, S. Development of the *Drosophila* retina, a  
1067 neurocrystalline lattice. *Dev Biol*. 1976;53(2):217-40.

1068 11. Cavener DR. Comparison of the consensus sequence flanking translational start sites  
1069 in *Drosophila* and vertebrates. *Nucleic Acid Res*. 1987;15(4):1353-61. PubMed Central  
1070 PMCID: PMC PMC340553.

1071 12. O'Neill EM, Ellis, M.C., Rubin, G.M., Tjian, R. Functional domain analysis of glass, a  
1072 zinc-finger-containing transcription factor in *Drosophila*. *Proc Natl Acad Sci U S A*.  
1073 1995;92(14):6557-61. PubMed Central PMCID: PMCPMC41557.

1074 13. Naval-Sanchez M, Potier, D., Haagen, L., Sanchez, M., Munck, S., Van de Sande, B.,  
1075 Casares, F., Chrisiaens, V., Aerts, S. Comparative motif discovery combined with  
1076 comparative transcriptomics yields accurate targetome and enhancer predictions. *Genome Res*.  
1077 2012;23(1):74-88. doi: 10.1101/gr.140426.112. PubMed Central PMCID: PMCPMC3530685.

1078 14. FlyBase. FlyBase inference based on genome sequence analysis. 1996.

1079 15. Annotators FG. Changes affecting gene model number or type in release 3.2 of the  
1080 annotated *D.melanogaser* genome. 2004.

1081 16. Jungreis I, Lin, M.F., Spokony, R., Chan, C.S., Negre, N., Victorsen, A., White, K.P.,  
1082 Kellis, M. Evidence of abundant stop codon readthrough in *Drosophila* and other metazoa.  
1083 *Genome Res*. 2011;21(12):2096-113. doi: 10.1101/gr.119974.110. PubMed Central PMCID:  
1084 PMCPMC3227100

1085 17. Belusic G. ERG in *Drosophila*2011.

1086 18. Silver S.J RI. Signaling circuitries in development: insights from the retinal  
1087 determination gene network. *Development*. 2005;132(1):3-13. doi: 10.1242/dev.01539.

1088 19. Jungreis I, Chan, C.S., Waterhouse, R.M., Fields, G., Lin, M.F., Kellis, M.  
1089 Evolutionary Dynamics of Abundant Stop Codon Readthrough. *Mol Biol Evol*.  
1090 2016;33(12):3108-32. doi: 10.1093/molbev/msw189. PubMed Central PMCID:  
1091 PMCPMC5100048.

1092 20. Lin MF, Carlson, J.W., Crosby, M.A., Matthews, B.B., Yu, C., Park, S., Wan, K.H.,  
1093 Schroeder, A.J., Gramates, L.S., St Pierre, S.E., Roark, M., Wiley, K.L. Jr., Kulathinal, R.J.,  
1094 Zhang, P., Myrick, K.V., Antone, J.V., Celniker, S.E., Gelbart, W.M., Kellis, M. Revisiting  
1095 the protein-coding gene catalog of *Drosophila melanogaster* using 12 fly genomes. *Genome*  
1096 Res. 2007;17(12):1823-36. doi: 10.1101/gr.6679507. PubMed Central PMCID: PMC  
1097 PMC2099591.

1098 21. Chittum HS, Lane, W.S., Carlson, B.A., Roller, P.P., Lung, F.D., Lee, B.J., Hatfield,  
1099 D.L. Rabbit beta-globin is extended beyond its UGA stop codon by multiple suppressions and  
1100 translational reading gaps. *Biochemistry*. 1998;37(31):10866-70. doi: 10.1021/bi981042r.

1101 22. Liang X, Mahato S, Hemmerich C, Zelhof AC. Two temporal functions of Glass:  
1102 ommatidium patterning and photoreceptor differentiation. *Developmental biology*.  
1103 2016;414(1):4-20. Epub 2016/04/24. doi: 10.1016/j.ydbio.2016.04.012. PubMed PMID:  
1104 27105580; PubMed Central PMCID: PMC4875859.

1105 23. Lykke-Andersen S, Jensen, T.H. Nonsense-mediated mRNA decay: an intricate  
1106 machinery that shapes transcriptomes. *Nat Rev Mol Cell Biol*. 2015;16(11):665-77. doi:  
1107 10.1038/nrm4063.

1108 24. Rio DC, Laski, F.A., Rubin, G.M. Identification and immunochemical analysis of  
1109 biologically active *Drosophila* P element transposase. *Cell*. 1986;44(1):21-32.

1110 25. Gontijo AM, Miguela, V., Whiting, M.F., Woodruff ,R.C., Dominguez, M. Intron  
1111 retention in the *Drosophila melanogaster* Rieske Iron Sulphur Protein gene generated a new  
1112 protein. *Nat Commun*. 2011;2(323). doi: 10.1038/ncomms1328. PubMed Central PMCID:  
1113 PMCPMC3113295.

1114 26. Wong JJ, Au, A.Y., Ritchie, W., Rasko, J.E. Intron retention in mRNA: No longer  
1115 nonsense: Known and putative roles of intron retention in normal and disease biology.  
1116 *Bioessays*. 2016;38(1):41-9. doi: 10.1002/bies.201500117.

1117 27. Kozak M. Pushing the limits of the scanning mechanism for initiation of translation.  
1118 *Gene*. 2002;299:1-34. doi: 10.1016/S0378-1119(02)01056-9.

1119 28. Kozak M. Regulation of translation via mRNA structure in prokaryotes and eukaryotes.  
1120 *Gene*. 2005;361:13-37. doi: 10.1016/j.gene.2005.06.037.

1121 29. McGeachy AM, Ingolia, N.T. Starting too soon: upstream reading frames repress  
1122 downstream translation. *EMBO J*. 2016;35(7):699-700. doi: DOI: 10.15252/embj.201693946.  
1123 PubMed Central PMCID: PMCPMC4818767

1124 30. Johnstone TG, Bazzini, A.A., Giraldez, A.J. Upstream ORFs are prevalent  
1125 translational repressors in vertebrates. *EMBO J*. 2016;35(7):706-23. doi:  
1126 10.15252/embj.201592759. PubMed Central PMCID: PMCPMC4818764

1127 31. Hsu MK, Chen, F.C. Selective constraint on the upstream open reading frames that  
1128 overlap with coding sequences in animals. *PLoS One*. 2012;7(11). doi:  
1129 10.1371/journal.pone.0048413. PubMed Central PMCID: PMCPMC3486843.

1130 32. Ladoukakis E, Pereira, V., Magny, E.G., Eyre-Walker, A., Couso, J.P. Hundreds of  
1131 putatively functional small open reading frames in *Drosophila*. *Genome Biol*.  
1132 2011;12(11):R118. doi: 10.1186/gb-2011-12-11-r118. PubMed Central PMCID:  
1133 PMCPMC3334604.

1134 33. Parks AL, Cook, K.R., Belvin, M., Dompe, N.A., Fawcett, R., Huppert, K., Tan, L.R.,  
1135 Winter, C.G., Bogart, K.P., Deal, J.E., Deal-Herr, M.E., Grant, D., Marcinko, M., Miyazaki,  
1136 W.Y., Robertson, S., Shaw, K.J., Tabios, M., Vysotskaia, V., Zhao, L., Andrade, R.S., Edgar,  
1137 K.A., Howie, E., Killpack, K., Milash, B., Norton, A., Thao, D., Whittaker, K., Winner, M.A.,  
1138 Friedman, L., Margolis, J., Singer, M.A., Kopczynski, C., Curtis, D., Kaufman, T.C.,

1139 Plowman, G.D., Duyk, G., Francis-Lang, H.L. Systematic generation of high-resolution  
1140 deletion coverage of the *Drosophila melanogaster* genome. *Nat Genet.* 2004;36(3):288-92.  
1141 doi: 10.1038/ng1312.

1142 34. Port F, Chen, H.M., Lee, T., Bullock S.L. Optimized CRISPR/Cas tools for efficient  
1143 germline and somatic genome engineering in *Drosophila*. *Proc Natl Acad Sci U S A.*  
1144 2014;111(29):E2967-76. doi: 10.1073/pnas.1405500111. PubMed Central PMCID:  
1145 PMCPMC4115528

1146 35. Gratz SJ, Cummings, A.M., Nguyen, J.N., HAm, D.C., Donohue, L.K., Harrison,  
1147 M.M., Wildogner J., O'Connor-Giles, K.M. Genome engineering of *Drosophila* with the  
1148 CRISPR RNA-guided Cas9 nuclease. *Genetics.* 2013;194(4):1029-35. doi:  
1149 10.1534/genetics.113.152710. PubMed Central PMCID: PMCPMC3730909.

1150 36. Gratz SJ, Ukken, F.P., Rubinstein, C.D., Thiede, G., Donohue, L.K., Cummings, A.M.,  
1151 O'Connor-Giles, K.M. Highly specific and efficient CRISPR/Cas9-catalyzed homology-  
1152 directed repair in *Drosophila*. *Genetics.* 2014;196(4):961-71. doi:  
1153 10.1534/genetics.113.160713. PubMed Central PMCID: PMCPMC3982687.

1154 37. Belusic G. ERG in *Drosophila*. In: Belusic DG, editor. *Electroretinograms*  
1155 IntechOpen; 2011.

1156 38. Nolo R, Abbott LA, Bellen HJ. Senseless, a Zn finger transcription factor, is necessary  
1157 and sufficient for sensory organ development in *Drosophila*. *Cell.* 2000;102(3):349-62. Epub  
1158 2000/09/07. PubMed PMID: 10975525.

1159

# Figure1

**A**  
 bioRxiv preprint doi: <https://doi.org/10.1101/537118>; this version posted January 05, 2019. The copyright holder for this preprint (which was not certified by peer review) is the author/funder, who has granted bioRxiv a license to display the preprint in perpetuity. It is made available under aCC-BY-ND 4.0 International license.

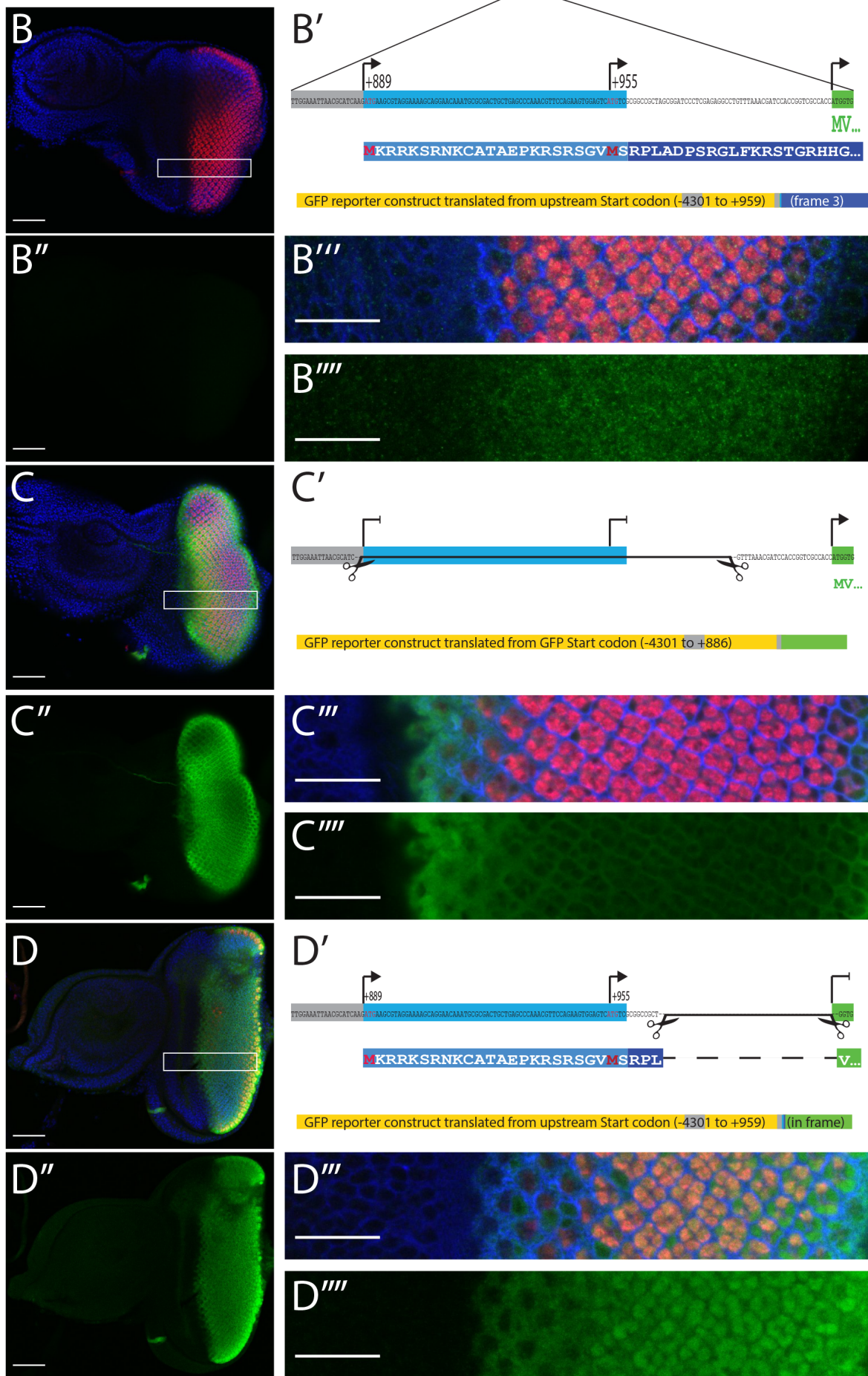
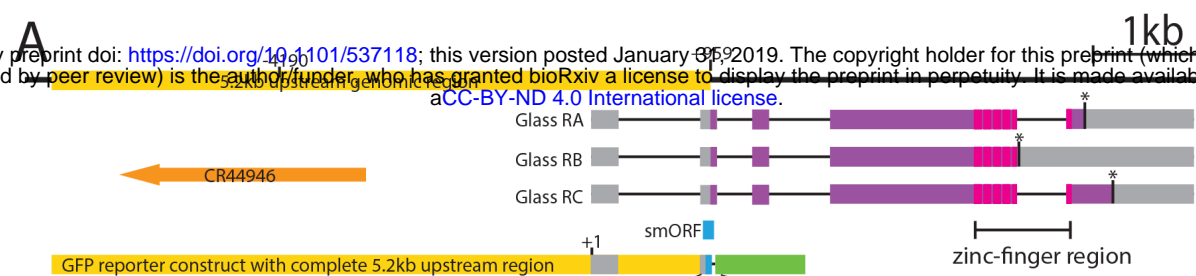


## Figure 2

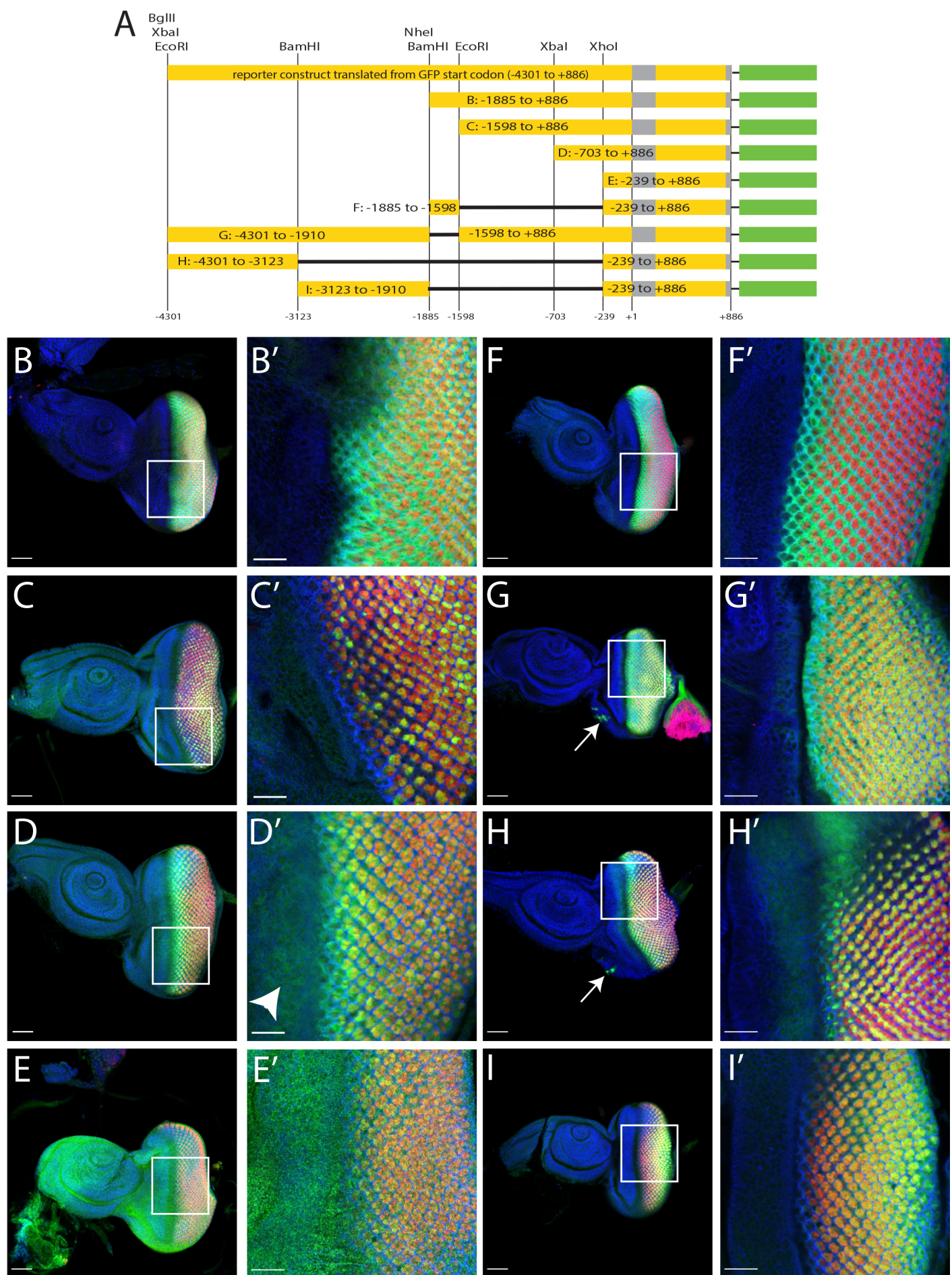
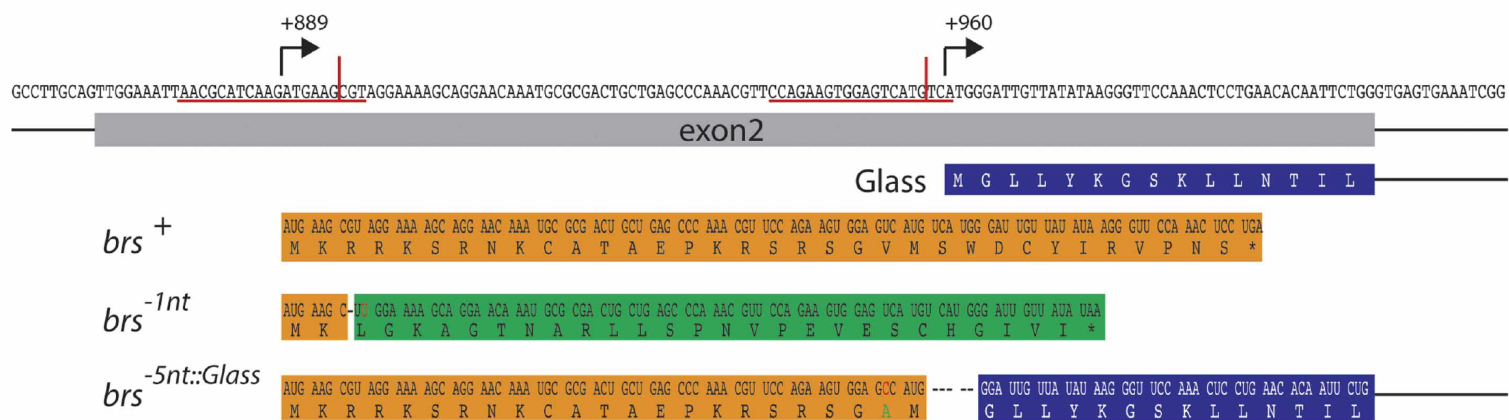


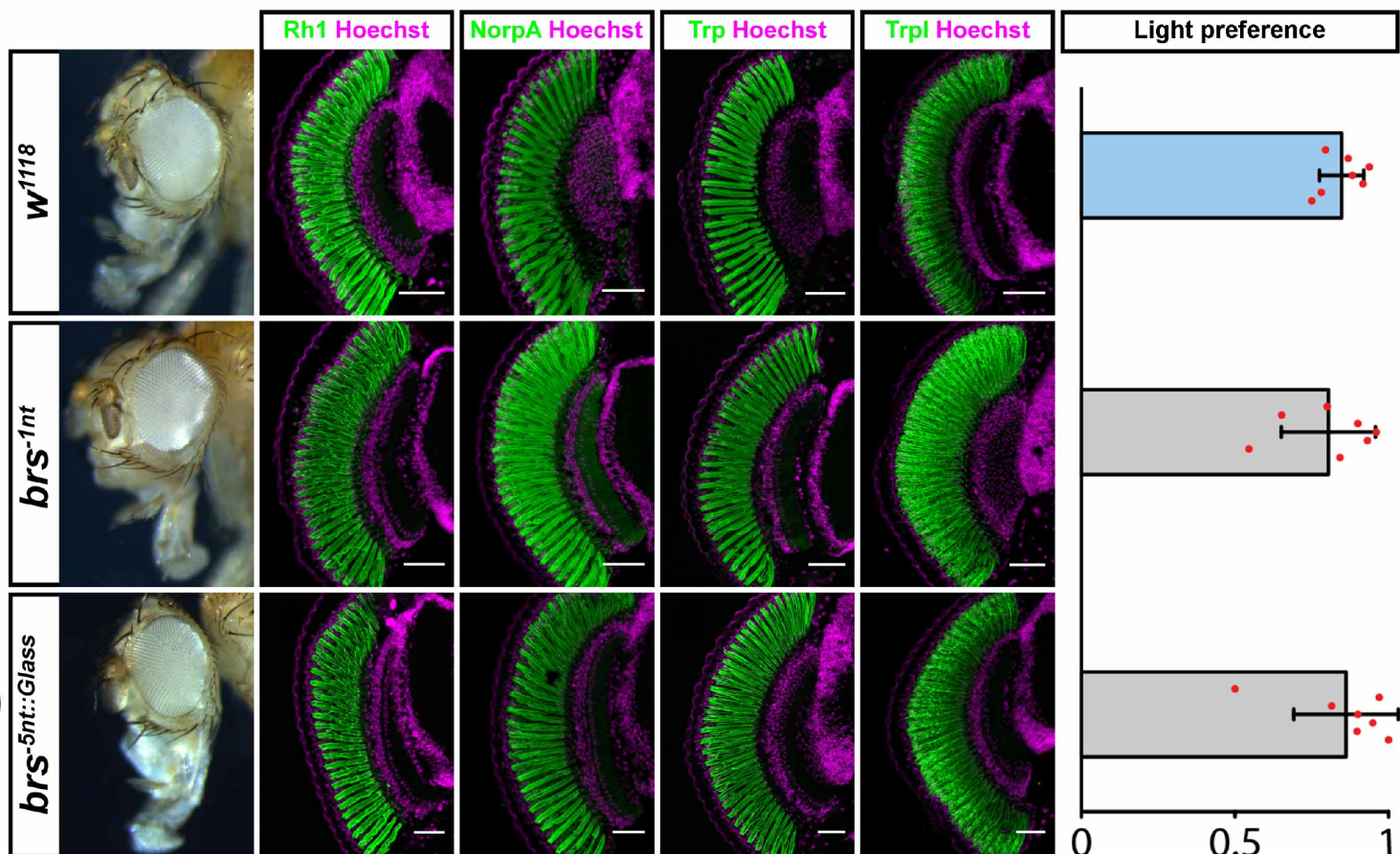
# Figure 3

bioRxiv preprint doi: <https://doi.org/10.1101/537118>; this version posted January 31, 2019. The copyright holder for this preprint (which was not certified by peer review) is the author/funder, who has granted bioRxiv a license to display the preprint in perpetuity. It is made available under aCC-BY-ND 4.0 International license.

A



B



D

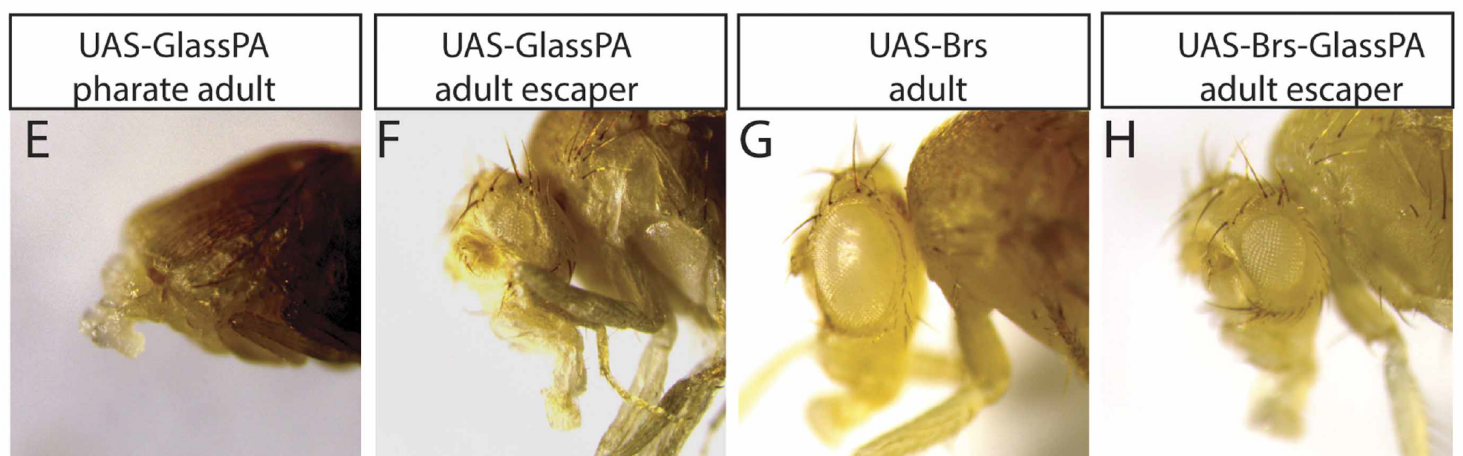
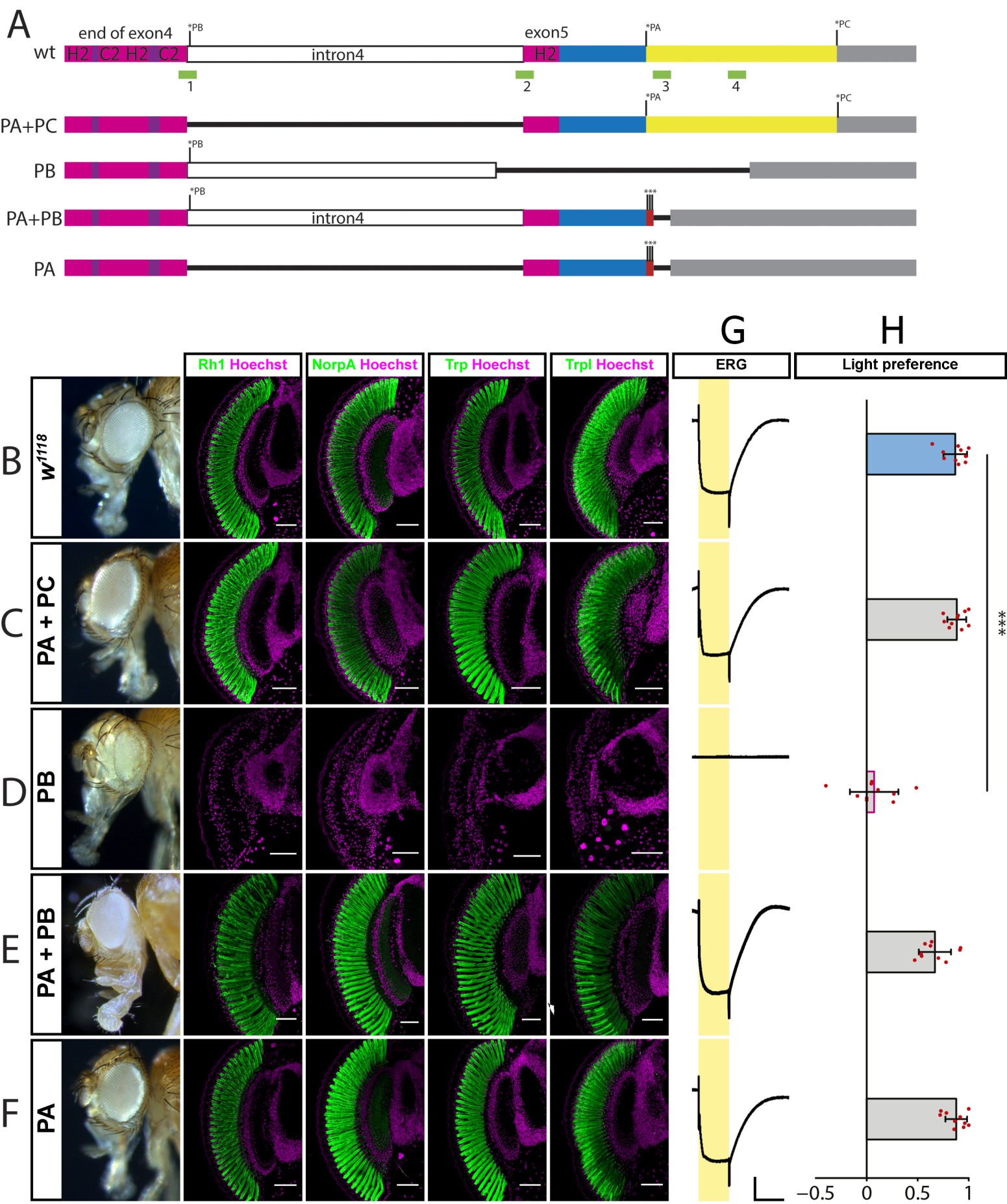


# Figure 4

bioRxiv preprint doi: <https://doi.org/10.1101/537118>; this version posted January 31, 2019. The copyright holder for this preprint (which was not certified by peer review) is the author/funder, who has granted bioRxiv a license to display the preprint in perpetuity. It is made available under aCC-BY-ND 4.0 International license.



UAS-constructs	# of <i>Cy<sup>+</sup></i> flies	# of <i>CyQ</i> flies	Total	Survival rate
<i>Glass-PA</i>	1	267	268	0.4%
<i>brs</i>	409	408	817	100.2%
<i>brs-glass-PA</i>	134	661	795	20.3%
<i>glass-PA; UAS-brs</i>	2	702	704	0.3%

**Table 1: *Brs* interferes with *Glass* translation.**

A strong *ey-Gal4/CyQ* driver line was crossed with different UAS-constructs and the number of *eclosed Cy<sup>+</sup>* and *CyQ* flies was determined. The *CyQ* siblings do not contain the *ey-Gal4* driver and therefore were taken as reference for the amount of *Cy<sup>+</sup>* flies expected in each experiment. The ratio of *Cy<sup>+</sup>* over *CyQ* flies determines the survival rate of flies expressing the UAS-construct.